Hexosamine Template. A Platform for Modulating Gene Expression and for Sugar-Based Drug Discovery

Noha Elmouelhi,[§,¶] Udayanath Aich,[§,#] Venkata D. P. Paruchuri, M. Adam Meledeo, Christopher T. Campbell, Jean J. Wang, Raja Srinivas, Hargun S. Khanna, and Kevin J. Yarema*

The Department of Biomedical Engineering, 106A Clark Hall, 3400 North Charles Street, The Johns Hopkins University, Baltimore, Maryland 21218

Received December 31, 2008

This study investigates the breadth of cellular responses engendered by short chain fatty acid (SCFA)−hexosamine hybrid molecules, a class of compounds long used in "metabolic glycoengineering" that are now emerging as drug candidates. First, a "mix and match" strategy showed that different SCFA (*n*-butyrate and acetate) appended to the same core sugar altered biological activity, complementing previous results [Campbell et al. *J. Med. Chem.* **2008**, *51*, 8135−8147] where a single type of SCFA elicited distinct responses. Microarray profiling then compared transcriptional responses engendered by regioisomerically modified ManNAc, GlcNAc, and GalNAc analogues in MDA-MB-231 cells. These data, which were validated by qRT-PCR or Western analysis for ID1, TP53, HPSE, NQO1, EGR1, and VEGFA, showed a two-pronged response where a core set of genes was coordinately regulated by all analogues while each analogue simultaneously uniquely regulated a larger number of genes. Finally, AutoDock modeling supported a mechanism where the analogues directly interact with elements of the NF-κB pathway. Together, these results establish the SCFA−hexosamine template as a versatile platform for modulating biological activity and developing new therapeutics.

Introduction

Our laboratory has established that amino sugars, primarily *N*-acetyl-D-mannosamine (ManNAc), developed by the metabolic glycoengineering community (see Figure 1 and reviews 1−3) have "scaffold-dependent" anticancer properties when derivatized by ester-linked SCFA[a] such as *n*-butyrate.[4,5] These newfound activities were manifest in the ability of C6-SCFA-appended, tributanoylated analogues such as 3,4,6-*O*-Bu_3ManNAc or 3,4,6-*O*-Bu_3GlcNAc (compounds **1b** and **2a**, Figure 2) to suppress proinvasive oncogenes that include MMP-9, MUC1, and CXCR4 and inhibit the mobility of metastatic MDA-MB-231 breast cancer cells.[5] In contrast to their comparable modulation of proinvasive oncogenes, these isomers diverged in their ability to induce apoptosis in cancer cells; the ManNAc analogue **1b** (or **1a**[6]) killed cells after about 2 weeks of exposure, while the corresponding GlcNAc analogue **2a** provided only transient growth inhibition that was relieved after 3−5 days.[4] The observation that these two compounds (**1b** and **2a**), which only differ in their core hexosamine, simultaneously held similar (evidenced by their effects on NF-κB[5]) and divergent biologic activities (shown by their impact on apoptosis[6]) had two implications. First, for metabolic glycoengineering, the generally accepted premise that this class of sugar analogues functioned as "silent" delivery vehicles for modifying the cell surface without unduly perturbing cellular metabolism required reevaluation. Second, and more positively, the scaffold-dependent activities raised the intriguing possibility that the core hexosamine structure could serve as a versatile template for drug discovery.

The premise that carbohydrates could be viable drug candidates runs counter to longstanding dogma that sugars are not "druggable"[7] because of factors such as insufficient stability and poor pharmacological characteristics (e.g., rapid serum clearance).[8,9] Nonetheless, accumulating evidence suggests that the stability of carbohydrate-based drugs is greater than generally appreciated, rendering these molecules appealing templates for the versatile positioning of functional groups in three-dimensional space.[10,11] Indeed, a recent review by Meutermans and coauthors outlined several classes of carbohydrates that have been used in ascendant drug development efforts over the past few years;[10] it was noteworthy, however, that hexosamines (the class of amino-containing monosaccharides widely used in metabolic glycoengineering experiments) were not included in these authors' compilation of sugar-based drug candidates. The purpose of this report is to fill this void by investigating how broadly hexosamines, when appended with ester-linked SCFA, modulate biological activity and thus have value as drug candidates.

One possibility, raised by the similar cellular responses elicited by ManNAc- and GlcNAc-based analogues when evaluated against a limited number of end points (metabolic flux, growth inhibition, and MUC1 expression[4]), was that the many possible structural variants of these molecules (Figure 2) would primarily support the two major modes of activity observed previously (i.e., high flux with low toxicity[4] or enhanced toxicity with suppression of prometastatic oncogenes[5]). At the other end of the spectrum, another possibility was that each structural modification would uniquely influence biological activity. To help resolve this issue in the current work,

* To whom correspondence should be addressed. Phone: 410-516-4914. Fax: 410-516-8152. E-mail: kyarema1@jhu.edu.

§ These authors contributed equally to this work.

¶ Current affiliation: Advanced Technologies & Regenerative Medicine, LLC, Somerville, NJ.

Current affiliation: 77 Massachusetts Ave, Bldg 16-561, Massachusetts Institute of Technology, Cambridge, MA 02139.

[a] Abbreviations: SCFA, short chain fatty acids; MMP-9, matrix metalloproteinase 9; MUC1, mucin 1; CXCR4, chemokine (C-X-C motif) receptor 4; NF-κB, nuclear factor κ B; SAR, structure−activity relationships; HDACi, histone deacetylase inhibitor; IC, inhibitory concentration; FC, fold change; ID1, inhibitor of DNA binding 1; NQO1, NAD(P)H dehydrogenase quinone 1; VEGFA, vascular endothelial growth factor A; TGF-β1, transforming growth factor β 1; EGR1, early growth response 1; TP53, tumor protein 53; HPSE, heparanase.

10.1021/jm801661m CCC: $40.75
Published on Web 03/27/2009

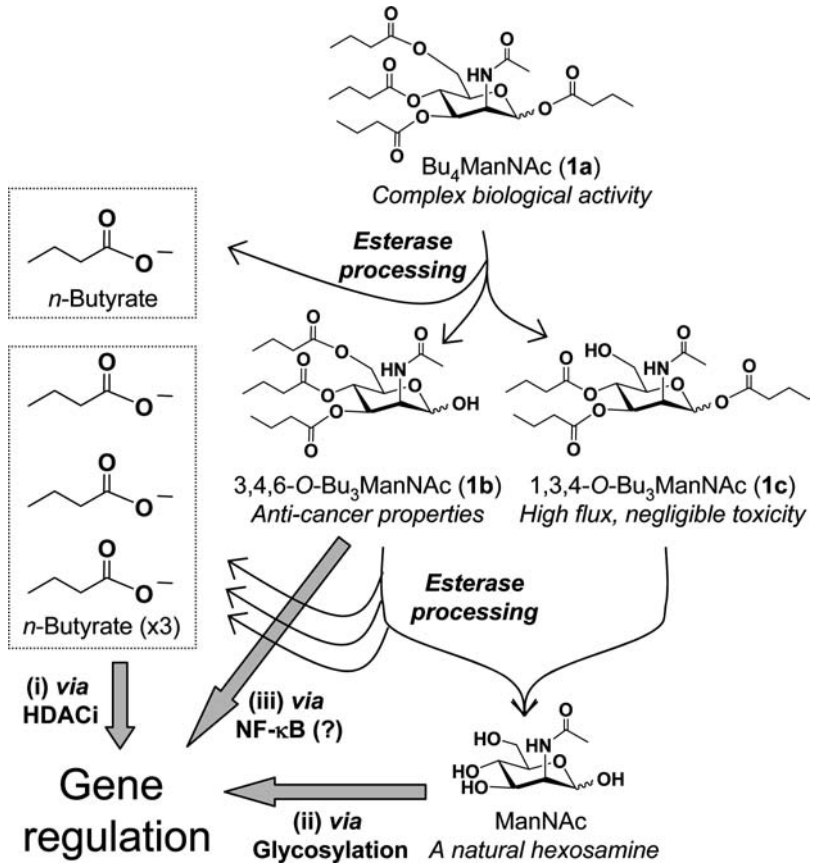

Figure 1. Overview of SCFA−hexosamine analogues, exemplified by the lead compound Bu_4ManNAc, used in metabolic glycoengineering and drug discovery. Esterases remove *n*-butyrate from Bu_4ManNAc (**1a**, top), producing tributanoylated derivatives that include 3,4,6-*O*-Bu_3ManNAc (**1b**) and 1,3,4-*O*-Bu_3ManNAc (**1c**), two isomers that have significantly different biological activities. Subsequent hydrolysis of the remaining three *n*-butyrate groups ultimately generates ManNAc, which is the dedicated precursor for sialic acid biosynthesis in mammalian cells, and an additional 3 equiv of *n*-butyrate. The net effect of the metabolism of this exemplar SCFA−hexosamine is to produce (i) *n*-butyrate that modulates gene expression through HDACi activity and (ii) ManNAc that impacts transcription through glycosylation-related mechanisms. In concert, providing a primary motivation of this study, (iii) a recently discovered third mechanism suggests that "anticancer" analogues with intact ester-linked SCFA (such as **1b**) modulate gene expression by engaging the NF-κB pathway while high flux, nontoxic analogues (such as **1c**) do not.

novel SCFA−hexosamine analogues were synthesized that supported the premise that *any* structural change made to these molecules tuned biological activity. Then to gain a wider perspective, mRNA profiling was used to probe structure−activity relationships (SAR) that include the composition of the *N*-acyl group and the regioisomeric placement of weakly active acetate or highly active *n*-butyrate SCFA moieties on each of the three major mammalian hexosamines (i.e., ManNAc, GlcNAc, and GalNAc, Figure 2A). The microarray data were validated by qRT-PCR and Western analysis of the mRNA and protein levels, respectively, of several cancer-related genes that responded to the panel of analogues. These results showed that the analogues coordinately regulated a small but significant number of genes while each compound also distinctively affected a substantially larger set of genes. Together, these experiments substantially increase the potential number of biological activities that can be modulated by SCFA−hexosamine analogues and establish these amino sugars as versatile templates for drug discovery. Finally, mechanistic insight into the activity of these molecules was gained from AutoDock modeling of the binding of analogues with anti-invasive properties to NFKB1, an element of the NF-κB pathway implicated in the cellular responses to these analogues.[5]

Results and Discussion

"Mix and Match" Analogues Tune Analogue Activity. The first experiments in this study explored an additional wrinkle in previously reported SAR where the presence (or absence) of an ester-linked acetyl or *n*-butanoyl substituent at the C1 or C6 position of a hexosamine (see Figure 1) was found to have a remarkable degree of control over biological activity.[4,5,12] In theory, the versatility of SCFA−hexosamine hybrid molecules would expand vastly if cellular responses could be controlled further by "mix and matching" different SCFA substituents on a single hexosamine scaffold. As a simple demonstration of this concept, three previously established end points (sialic acid production,[13] growth inhibition,[6] and MUC1 expression[4]) were compared in cells incubated with 6-*O*-Bu-1,3,4-*O*-Ac_3ManNAc (**1g**), and 1-*O*-Bu-3,4,6-*O*-Ac_3ManNAc (**1h**). These isomers both bear three acetyl and one *n*-butanoyl groups, but they differ in the positioning of *n*-butyrate on the core monosaccharide template with this four-carbon SCFA situated at the C6 position for **1g** and at the C1 position for **1h**.

The amount of sialic acid produced by cells incubated with either **1g** or **1h** was approximately equivalent to the perbutanoylated analogue **1a** and significantly higher than for the peracetylated counterpart **1d** (Figure 3A). This result showed that the replacement of a single acetate of peracetylated ManNAc (Ac_4ManNAc, **1d**) with *n*-butyrate substantially improved cellular uptake of the core sugar ManNAc when measured by sialic acid production (ManNAc is a dedicated metabolic intermediate for sialic acid biosynthesis,[14] and our previous experiments have shown that levels of this sugar closely correspond to ManNAc uptake in the absence of toxicity[13,15,16]).

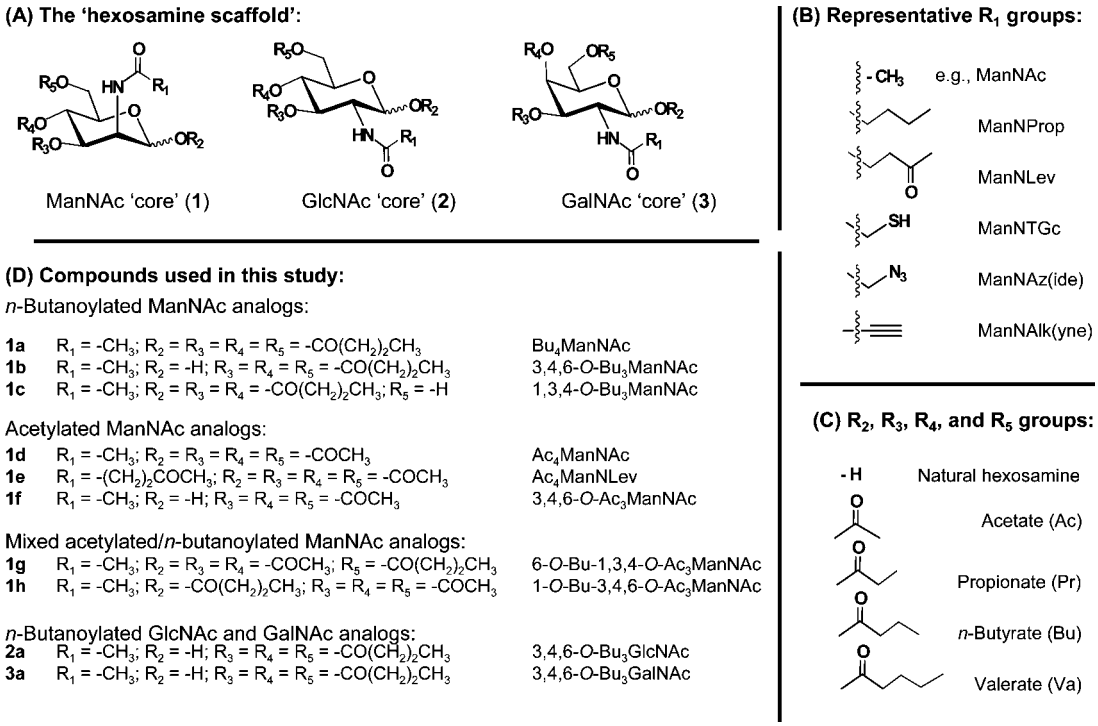

Figure 2. Hexosamine template, a platform for drug discovery. (A) The three common mammalian hexosamines (e.g., *N*-acetyl-D-mannosamine, ManNAc, *N*-acetyl-D-glucosamine GlcNAc, and *N*-acetyl-D-galactosamine GalNAc) are shown (R_1 = CH_3 and R_2, R_3, R_4, and R_5 = H for the natural sugars). These hexosamines can be derivatized with the ~25 "R_1" groups used in metabolic engineering (a sample of these are shown in panel B with names given based on a ManNAc "core"), and the R_2, R_3, R_4, and R_5 positions can be derivatized with any of the SCFA shown in panel C (longer-chain acyl groups render the hybrid molecules insoluble in aqueous medium). Together, this platform can supply tens of thousands of compounds (e.g., [3 hexosamines] × [2 anomers (α/β)] × [25 R_1 groups] × [5 R_2 groups] × [5 R_3 groups] × [5 R_4 groups] × [5 R_5 groups] = 93 750 different molecular species). The limited subset of these molecules tested in this study is given in panel D.

Moreover, the comparable level of sialic acid produced by **1g** and **1h** at subcytotoxic levels served as an internal control to ensure that roughly equivalent amounts of each analogue had been taken up by the cells, subsequently deprotected by esterases, and ultimately incorporated into the sialic acid pathway. Consequently, the significant difference in the growth rates of cells exposed to the more cytotoxic analogue **1g** and the less inhibitory analogue **1h** (Figure 3B) cannot be attributed to the trivial explanation that **1g** was taken up by a cell with greater efficiency. Instead, the results were consistent with the presence of the highly active *n*-butyrate SCFA at the C6 position, which was previously identified as a critical SAR for the "anticancer" effects of analogues.[4,5] The impact of each analogue on MUC1 production was also informative, with the C6-butanoylated compound **1g** showing approximately the same degree of suppression of this prometastatic oncogene as the peracetylated parent molecule **1d**; by contrast the C1-butanoylated compound **1h** had a negligible impact on MUC1 up to the highest test concentration of 400 μM (Figure 3C).

The significance of the disparate cellular responses to **1g** and **1h** in the context of exploiting the hexosamine scaffold to modulate biological activity during metabolic glycoengineering experiments or as a template for drug discovery was 2-fold. First, the differences between these two isomers verified the previous postulate that inherent features of the intact SCFA−sugar structure are important determinants of bioactivity.[4] As discussed in more detail elsewhere,[4,5,12] these results overturn the long held assumption that the activity of SCFA−monosaccharide hybrid molecules is solely derived from their hydrolysis products after processing by serum or intracellular esterases and lipases. Second, these results established that biological activity could be controlled by the copresentation of different SCFA on the same scaffold, extending previous observations made based on the presence (or absence) of a single type of ester-linked SCFA. This point is illustrated by the roughly similar abilities of **1d** and **1g** to suppress MUC1 expression while they diverged in their capacity to support sialic acid production and inhibit cell growth (**1g** was superior in both measures). By contrast, comparing **1h** to **1d** reveals that an *n*-butyrate group at the C1 position lessens both MUC1 suppression and growth inhibition but leaves the enhanced sialic acid production unchanged. These results show that, depending on its placement on the core sugar template, a single *n*-butyrate group has an intriguing ability to enhance or suppress distinct cellular responses.

SAR Analysis of SCFA−Hexosamine Analogues by Transcriptional Profiling. The finding that a relatively modest structural change (e.g., the substitution of a single acetate of **1d** with the *n*-butyrate found in **1g** or **1h**) had a measurable impact on biological activity opens the door to a combinatorial approach to SCFA−hexosamine drug discovery where the thousands of structural variants possible through R_1, R_2, R_3, R_4, and R_5 permutations (see Figure 2) could be exploited to individually tune cellular responses. To evaluate this possibility, it was clear that an expanded set of end points was required beyond the modest set of genes (e.g., MUC1, MMP-9, CXCR4, and NFKB1[5]) and cellular behaviors (growth inhibition, apoptosis, and invasion[4−6]) evaluated in our previous experiments. We therefore opted to use transcriptional profiling to compare cellular responses elicited by a selected panel of analogues to gain a broader sense of whether they simply co-regulated a similar set of genes (albeit potentially to different degrees, thereby explaining differences in cell-level responses) or whether each analogue provided a unique signature of gene expression.

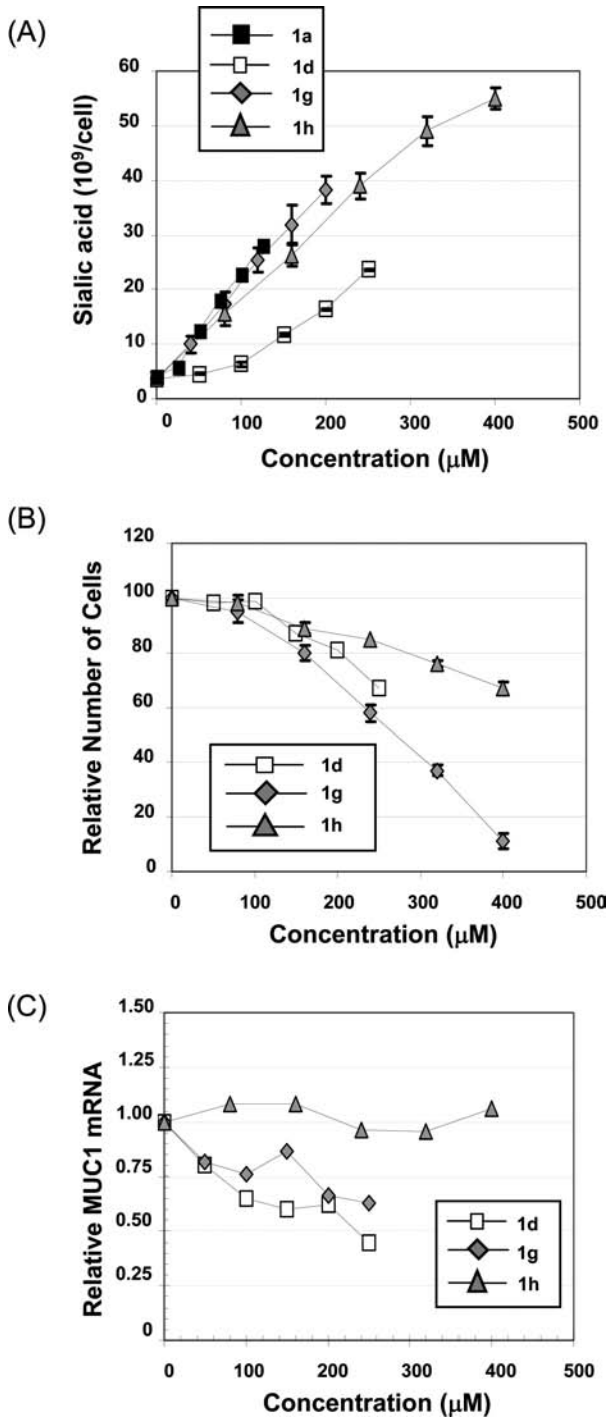

Figure 3. Biological activities of "mix and match" analogues. The impact of ManNAc analogues uniformly derivatized with *n*-butyrate (**1a**) or acetate (**1d**) was compared with two novel monobutanolylated, triacetylated isomers (**1g** and **1h**) on (A) sialic acid production, (B) growth inhibition, and (C) MUC1 expression in MDA-MB-231 cells using previously described methodology.[4,5] In panels A and B error bars represent the standard error of the mean (SEM) from a minimum of three independent experiments. In panel C, representative qRT-PCR data from one of three independent experiments are shown; each data point represents four determinations (error bars are omitted because they are typically smaller than the data symbol).

Effect of the *N*-Levulinoyl Group of Ac_4ManNAc Determined by GLYCOv3 Evaluation. The first set of mRNA profiling experiments compared the highly cytotoxic,[13] peracetylated analogue Ac_4ManNLev (**1e**) with peracetylated "natural" ManNAc (i.e., Ac_4ManNAc, **1d**); the structural difference between these two compounds lay in the *N*-acyllevulinoyl group used to install ketones into surface sialosdes.[17,18] Upon uptake into a cell, hydrolysis of the ester linkages of either compound produces 4 equiv of acetate, which is a weakly acting HDACi not anticipated to have a large impact on transcription at the micromolar concentrations used. As a consequence, a comparison of these compounds with the glycosylation-specific GLYCOv3 microarray developed by the Consortium for Functional Glycomics (CFG) was expected to highlight sugar-specific responses. Profiling of cells incubated with 100 μM of either compound showed that the analogues modulated a modest subset of glycosylation-related genes (~1% and 6% of ~1200 probe sets were affected by **1d** and **1e**, respectively; Figure 4A). Furthermore as expected, the ~6-fold higher level of genes regulated by **1e** clearly indicated the importance of the core sugar in defining the effects of the analogues on gene expression.

Despite establishing these important points, these results also left several issues not fully addressed. For example, the absolute number of genes regulated by these compounds was similar to those reported elsewhere to be modulated by SCFA (i.e., $\leq$5% of gene sets as measured in a previous microarray study of *n*-butyrate[19]). The different number of genes affected by each analogue, however, discounted a SCFA effect because the equivalent amount of acetate delivered by 100 μM of either analogue should have supported similar responses if hydrolyzed SCFA were primarily responsible for biological activity. On the basis of the likelihood that hydrolyzed acetate did not play a dominant role in the activity of either analogue, glycosylation-based explanations were entertained for the larger impact of the "Lev" group of **1e** on mRNA levels compared to the smaller set of genes impacted by **1d**. For example, **1e** reduces flux through the sialic acid pathway,[13] whereas **1d** dramatically increases flux.[16] On the basis of experimental precedent provided by "ManNProp"[20] and modeling simulations of flux-related changes to glycan biosynthesis,[21−23] it is likely that hexosamine analogues change the "sugar code" molecular recognition features of the cell surface[24] through changes to the branching status of *N*-glycans,[23,25] through changes to sialylation,[26] or through the incorporation of the "Sia5Lev" sialoside into surface elements.[17,18] As a result, it is plausible that effects extend to downstream signaling responses that engage transcription, thereby explaining the enhanced ability of **1e** to modulate transcription compared to **1d**.

Despite plausible glycosylation-based explanations for the greater impact of **1e** compared to **1d**, an important caveat was that these results might have been biased by the use of the GLYCOv3 microarray that did not monitor the entire global set of mRNAs. Another caveat was that the increased impact of **1e** could have been a consequence of the enhanced cytotoxicity compared to **1d**[13] that triggered apoptotic transcriptional programs in cells treated with the former compound. To avoid these pitfalls, subsequent experiments used the larger probe set available with the Affymetrix U133 2.0 Plus Array to determine if mRNA profiles affected by each analogue were biased toward glycosylation genes or whether they were more broadly distributed throughout the entire genome. In addition, care was taken to avoid artifactual changes to mRNA levels potentially introduced by the differential cytotoxicity of the various analogues by normalizing the levels of the "toxic" analogues to inhibit growth to 70% (IC_{70}) of nontreated controls.

Evaluation of Ac_4ManNLev (1e) with the Affymetrix Human Genome U133 2.0 Plus Array. To obtain a more complete picture of the genetic effects of hexosamine analogues than possible with the GLYCOv3 array, we next evaluated

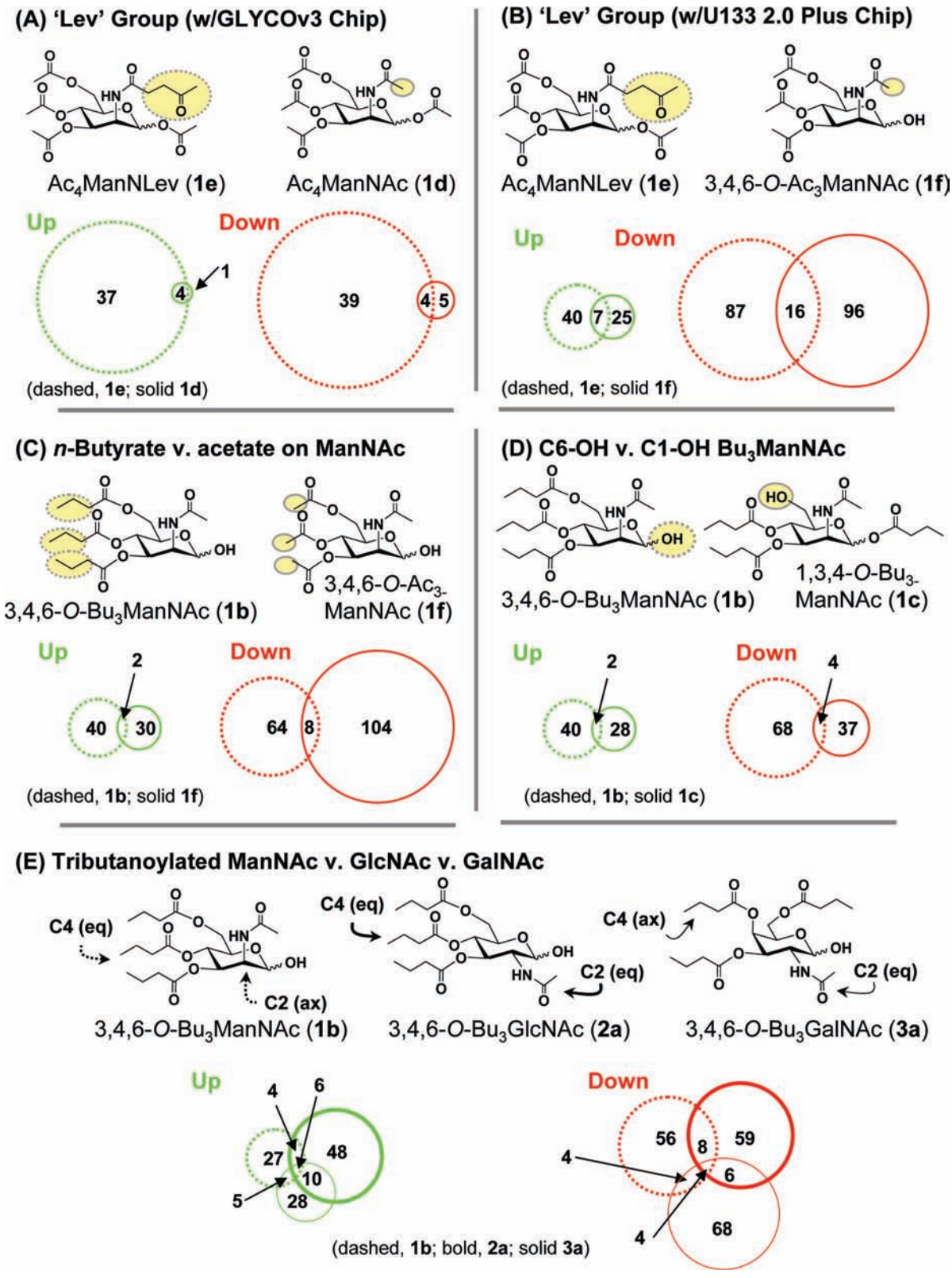

Figure 4. SCFA−hexosamine hybrid molecules elicit unique patterns of gene regulation. Microarray data (from the GLYCO3 array for panel A and from the Affymetrix U133 2.0 Plus chip for panels B−E) were compared for the indicated pairs (or triplet, panel E) of analogues. Key structural differences selected to probe various SAR for each set of compounds are highlighted by the dashed and solid ovals, and the overlapping and distinct number of genes that were up- or down-regulated in each case are given in Venn diagrams.

mRNA levels by using the Affymetrix Human Genome U133 2.0 Plus chip, a comprehensive microarray chip with over 50 000 probe sets. This chip provided information on the expression of the majority of human genes, not just the set of glycosylation-related transcripts analyzed by the GLYCOv3 chip. In the first experiments with the U133 2.0 Plus chip, we re-evaluated Ac_4ManNLev (**1e**) and compared it to 3,4,6-*O*-Ac_3ManNAc (**1f**). The reason for using this triacetylated form of ManNAc instead of **1d** was that we sought to use equitoxic concentrations of each compound, and on the basis of concurrent discoveries,[4]

C1-OH triacetylated analogues proved to be more toxic than their peracylated counterparts and thus more suited for comparison with the "Lev" analogue. In addition, both compounds were ester derivatized at the C6 position, a critical SAR that contributes to cytotoxicity.[5] Consequently, these analogues provided an acceptable comparison of the *N*-acetyl group of **1f** with the *N*-levulinoyl group of **1e**, making it instructive that the expanded U133 2.0 Plus probe set showed that **1e** regulated approximately the same number of genes as **1f** (Figure 4B) rather than the ~6-fold higher level previously observed in comparison with **1d**.

The simplest explanation for the much smaller disparity in the *number* of genes modulated by the *N*-levulinoyl and *N*-acetyl analogues **1e** and **1f** when they were analyzed by the U133 2.0 Plus chip compared to the GLYCOv3 chip was that carefully controlling for cytotoxicity leveled the responses to each analogue. This surface explanation, however, could not account for disparate identities of the genes regulated by each compound (Figure 4B). Interestingly, both analogues down-regulated more genes than they up-regulated, which was inconsistent with the protranscription, open chromatin form promoted by increased histone acetylation in SCFA-treated cells, thereby diminishing the role of hydrolyzed acetate (in which case both analogues should have elicited similar behavior). Instead, these results pointed toward a dominant role for the core sugar in specifying the transcriptional responses to **1d**, **1e**, and **1f**.

Evaluation of the Acetylation of ManNAc Compared to *n*-Butanoylation. As just discussed, a dominant role for hydrolyzed acetate groups was discounted by the microarray results comparing **1d**, **1e**, and **1f**. One limitation of evaluating acetylated analogues for SCFA responses, however, was the relatively weak HDACi activity of acetate compared to longer chain SCFA such as *n*-butyrate. Therefore, to more conclusively establish that SCFA played only a minor role, we attempted to amplify latent transcriptional responses by comparing 3,4,6-*O*-Ac_3ManNAc (**1f**) with 3,4,6-*O*-Bu_3ManNAc (**1b**). The latter compound was derivatized with the highly active *n*-butyrate SCFA, and if SCFA effects had been overlooked because of the weak activity of acetate, this shortcoming would be overcome with **1b**. Consistent with HDACi activity, the tributanoylated analogue **1b** did up-regulate a slightly higher number of genes than its triacetylated counterpart **1f** (**42** vs **32**; Figure 4C); however, the enhanced activity of **1b** did not carry over to the number of genes that were down-regulated where **1b** lagged **1f** by 112 to 72. Overall, the relatively minor number of genes co-regulated by both compounds (10 of 250, or 2%) was consistent with reports that various SCFA (e.g., free acetate, propionate, and *n*-butyrate) each have a distinct impact on gene expression.[27] Inconsistent with an HDACi effect, however, more genes were once again down-than up-regulated, which is at odds with the expected protranscriptional propensity of the HDACi. These results, therefore, provide added support for the premise that SCFA gain a novel and general ability to modulate gene expression when presented on a hexosamine scaffold.

Comparison of the C1-OH vs C6-OH Isomers of Tributanoylated ManNAc. To further probe the relative contributions of the HDACi activity of *n*-butyrate to modulate gene expression when presented to cells on a hexosamine scaffold, the mRNA profile of 3,4,6-*O*-Bu_3ManNAc (**1b**) was compared with its C6-OH isomer 1,3,4-*O*-Bu_3ManNAc (**1c**). In this case, equimolar amounts of *n*-butyrate were delivered by each compound, which should result in identical expression profiles from the hydrolyzed SCFA. Accordingly, the differences seen between the two compounds, where the C1-OH isomer **1b** had a greater impact on transcription than the C6-OH isomer **1c** (Figure 4D), are attributable to template dependent responses. Again, the number of genes co-regulated by both analogues was a relatively small proportion of the total with only two genes up- and four down-regulated in common. This comparison unambiguously established that features of the intact SCFA−hexosamine molecule, in particular (but not necessarily limited to) the presence or absence of a SCFA group at the C1 or C6 position, were critical determinants of the diverse transcriptional impact of acylated hexosamines. Combined with the effects of the *N*-acyl group (i.e., "R_1" in Figure 2 and "Lev" in Figure 4, panels A and B), these experiments provided convincing proof that ManNAc is an appropriate molecular scaffold for modulating biological activity through structural features of the intact SCFA−hexosamine linkages and discounted the roles for the hydrolyzed sugar and *n*-butyrate or acetate moieties.

Comparison of C1-OH Tributanoylated ManNAc, GlcNAc, and GalNAc. The experiments described above evaluated the presentation of SCFA on a ManNAc (or *N*-acyl modified ManNLev) scaffold and unequivocally established that structural features of the intact hybrid molecules dominated biological activity. In the last set of SAR comparisons, we evaluated all three of the common mammalian hexosamines (i.e., GlcNAc and GalNAc as well as ManNAc) to ask whether transcription could be governed further by the stereochemistry of the C2 or C4 positions of the monosaccharide template. The subsequent mRNA profiling of cells treated with 3,4,6-*O*-Bu_3ManNAc (**1b**), 3,4,6-*O*-Bu_3GlcNAc (**2a**), and 3,4,6-*O*-Bu_3GalNAc (**3a**) showed that each analogue again elicited distinct patterns of gene expression with relatively minimal overlap between analogues (Figure 4E).

The Broader Significance of the Microarray Profiling. The "Big Picture". A Comparison of Transcriptional Patterns Reveals Persistent and Statistically Improbable Similarities. The various comparisons of transcriptional responses to analogues obtained from the U133 2.0 Plus gene chip analyses (in Figure 4B−E) demonstrated that the type of SCFA (e.g., acetate vs *n*-butyrate), type of sugar core (ManNLev vs ManNAc; ManNAc vs GlcNAc vs GalNAc), and even the regioisomeric placement of the SCFA on the core sugar (e.g., 1,3,4-*O*-Bu_3ManNAc vs 3,4,6-*O*-Bu_3ManNAc) all have the ability to tune biological activity. In each of these comparisons, a substantially larger number of genes were uniquely affected by one or the other of the analogues rather than being regulated in tandem. However, by use of the rudimentary statistical analysis presented below, even the relatively small number of genes that were coordinately regulated could not have occurred randomly, thus suggesting that the analogues, as part of their ability to modulate transcription, impinge on a common regulatory mechanism.

The roughly similar total number of genes regulated by each of the C6-SCFA derivatized analogues (between ~110 and ~150, Figure 5A) provided a first line of evidence that a common set of regulatory mechanisms might determine transcriptional responses to the analogues. Evidence to the contrary, however, lay in the observation that 5% or fewer genes were typically coordinately regulated when any two analogues were compared (Figure 5B, first four sets of columns correspond to the data shown in Figure 4, panels B, C, D, and E, respectively). The relatively low overlap was somewhat surprising considering that the comparisons had been made between analogues selected for closely matched SAR. Interestingly, ignoring SAR that emphasized similarities and comparing the two most dissimilar analogues, Ac_4ManNLev (**1e**) and 3,4,6-*O*-Bu_3GlcNAc (**2a**),

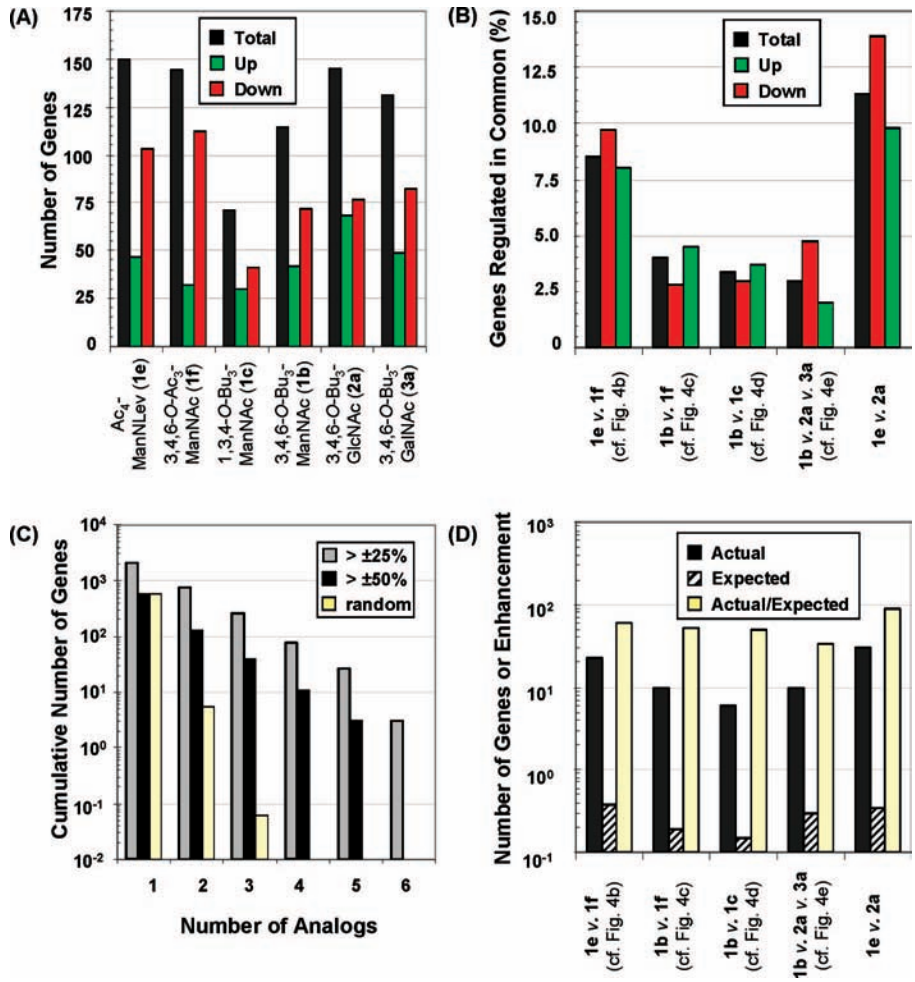

Figure 5. Summary and analysis of the number of genes regulated by the various analogues. (A) The total number of genes impacted, as well as those specifically up- or down-regulated, by each of the analogues analyzed by the U133 2.0 Plus chip is shown. (B) The percentage of genes regulated in common (compared to the total of number of genes affected by each pair or set of analogues) is shown. (C) The total number of genes regulated by more than 25% or 50% (either up or down) by the indicated number of analogues is shown; for example, 573 genes were regulated by >50% by any one analogue (as shown in the column indicated by the "1") but no genes were regulated by >50% by all six analogues (as shown in the column indicated by the "6"). For a threshold of >25% change, 2062 genes were regulated by any one analogue, a number that diminished to 3 for co-regulation by all six analogues. (D) The actual number of genes co-regulated by the indicated sets of analogues (either up- or down-, as indicated by the black bars) was much higher than expected if gene changes occurred entirely at random (crosshatched bars). The fold-enhancement is given as the ratio of the actual results to those expected from a random distribution of genes.

which bore different *N*-acyl groups and configuration (i.e., axial vs equatorial), as well as different *O*-hydroxyl modifications, showed that the percentage of genes (≥10%) co-regulated by these two analogues was greater than in any other comparison (Figure 5B, rightmost set of data).

The fact that a "random" comparison of analogues revealed the largest number of coordinately regulated genes led to a rudimentary statistical evaluation of what would be expected if genes were regulated randomly (i.e., by completely independent mechanisms) by each analogue. As shown in Figure 5C, the number of genes regulated in common by increasing numbers of analogues decreased less rapidly than expected if each analogue regulated a random set of genes. Specifically, on the basis of the total of 573 different transcripts being regulated by ±50% by any analogue (±50% fold-change or FC), there was ∼ 1% probability that any one of the ∼50000 probe sets would be affected by an analogue. If these genes were randomly distributed across genome space, about five would be expected to be co-regulated by any two analogues (i.e., 0.01 × 0.01 × 50 000) and there would be less than a 0.0001% chance that *any* gene would be simultaneously affected by three analogues. The fact that several genes are co-regulated by the statistically improbable combinations of four or five (or even six at ± 25% FC) analogues indicates that the transcriptional effects of individual analogues are not completely random but rather share a common mechanism.

A final analysis of each comparison made in Figure 4 (as shown in Figure 5D) reveals that the actual number of coordinately regulated genes is much greater than the number expected based on random distribution. To explain this data with one example, a comparison of Ac_4ManNLev (**1e**) with 3,4,6-*O*-Ac_3ManNAc (**1f**) showed that 23 genes were regulated in common by both analogues. This number was much higher than expected on the basis of the regulation of 150 genes by **1e** (0.27% of all genes on the chip) or 144 genes (0.26% of all genes) by **1f**. If these genes were randomly distributed throughout genome space, there would be a 0.0702% (0.0027 × 0.0026) likelihood of coordinate regulation of any gene, and on the basis of the total number of genes on the array, **1e** and **1f** would be expected to co-regulate less than one (specifically 0.38) gene. Thus, because 23 genes were experimentally found to be co-regulated, the actual number of genes regulated in common was enhanced ∼61-fold over the number expected if there were no coordination between the analogues. A similar analysis for each

Table 1. List of Pathways Identified from the Pathway Express Software Analysis of the Microarray Profiling Data

pathway name	impact factor	genes in pathway	input genes in pathway	pathway genes on chip
leukocyte transendothelial migration	8.400	117	9	115
complement and coagulation cascades	6.764	69	5	67
apoptosis	6.147	84	6	84
epithelial cell signaling in *Helicobacter pylori* infection	6.022	46	3	45
Wnt signaling pathway	5.148	147	8	145
focal adhesion	5.114	194	9	193
tight junction	5.111	119	7	118
regulation of autophagy	4.868	29	3	25
gap junction	4.323	99	5	97
toll-like receptor signaling pathway	4.268	91	5	88
cell adhesion molecules (CAMs)	4.013	132	6	128
adipocytokine signaling pathway	4.008	69	4	68
axon guidance	3.381	130	6	129
type I diabetes mellitus	3.350	44	3	40

set of comparisons reveals comparable enhancements of ~33- to 90-fold in each case (Figure 5D).

Pathway Analysis Shows Relationships Consistent with Known Biologic Responses to Analogues. As suggested by the evaluation of other end points in previous studies and confirmed in the mRNA profiling described above, the gene-regulatory properties of SCFA−hexosamine hybrid molecules are overwhelming defined by features of the intact molecule rather than by hydrolysis products. As a consequence, responses to these molecules are highly specific and depend on the exact combination of a core sugar with an SCFA of a specific chain length as well as the regioisomeric placement on the core sugar (Figure 4). At the same time, the genes regulated in common by the various combinations of analogues were present at a much higher frequency than would be expected from a random distribution (Figure 5), suggesting that the hexosamine core structure, while highly tunable, provides a platform to modulate a "core" set of biological activities. In order to gain a sense of the coordinate activities held by this class of analogues, we used the Pathway-Express software tools[28] to predict signaling networks or biochemical pathways affected by the analogues (Table 1). The networks that were identified were qualitatively consistent with results we have observed previously where the Wnt signaling pathway and cell adhesion were affected by metabolic glycoengineering analogues[29] and cell migration was altered by anticancer analogues such as **1a** and **1b** used in this report.[5]

Development of a Network of Cancer-Related Genes Impacted by the Analogues. A particularly pertinent result of the Pathway-Express software analysis was the high ranking of the apoptosis pathway based on our past findings that analogues such as Ac_4ManNLev (**1e**),[13] Bu_4ManNAc (**1a**),[6] and 3,4,6-*O*-Bu_3ManNAc (**1b**)[4] were apoptotic in cancer cells; previously, however, we had little molecular level insight into the mechanism through which the analogues executed apoptosis. Consequently, it was highly significant that we could begin to fill this void by assembling the coordinately regulated genes into the network shown in Figure 6. An important feature of this network is that it includes not only genes involved in apoptosis but also previously unidentified elements that regulate the mobility of cells, thereby augmenting the anti-invasive mechanisms that we previously associated with the modulation of MMP-9 and MUC1.[5]

Biochemical Validation of the Microarray Results by qRT-PCR and Western Analysis. Quantitative Real-Time PCR (qRT-PCR) Validation of Selected Gene Targets. The microarray profiling and subsequent data analysis provided important new insights into the anticancer properties of SCFA−hexosamine drug candidates. However, the changes in gene expression were typically rather modest (albeit statistically significant) because of the low concentrations of analogue used to avoid secondary responses associated with cytotoxicity. Consequently, we used qRT-PCR to thoroughly validate transcriptional changes identified through microarray profiling. The specific genes selected for analysis (ID1, NQO1, VEGFA, and TGF-β) were chosen for several reasons. For example, ID1 was down-regulated by five analogues (all of the C6-acyl derivatized compounds) and is a promising target in cancer therapy.[30] Similarly, NQO1 and VEGFA were selected on the basis of their involvement in networks that regulate apoptosis in cancer cells (see Figure 6), an end point that *n*-butanoylated analogues were previously found to influence.[4,6] TGF-β1 was a negative control of sorts; while it was expressed in the target cells and is involved in the network of genes that involve NQO1 and VEGFA, it was not directly modulated by the analogues in the microarray profiling experiments.

Once genes were selected for detailed validation, analogues chosen for these tests were narrowed to the "active" C1-OH form of tributanoylated ManNAc **1b** and the corresponding "inactive" C6-OH isomer **1c**. At the outset, **1b** was predicted to have a greater impact than **1c** (and was thus deemed as "active") on the selected cancer-related genes based on SAR that a C6-substituent was necessary to induce apoptosis and suppress MUC1.[4] This prediction was fulfilled for ID1 (Figure 7A), VEGFA (Figure 7B), and NQO1 (Figure 7C), while neither analogue had a statistically significant effect on TGF-β1 expression (Figure 7D). In these experiments, concentrations

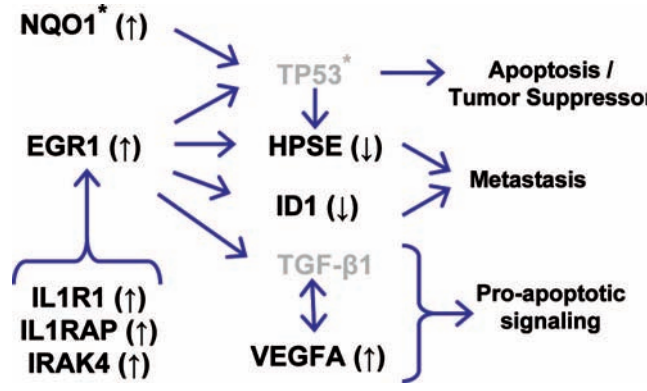

Figure 6. Network of cancer-related genes identified from the mRNA profiling experiments. The analysis is based on ±25% changes in expression elicited by all analogues in MDA-MB-231 cells. The * symbol indicates genes that are mutated in MDA-MB-231 cells, and elements indicated in gray are not changed with statistical significance in the microarray data (but are indicated in the chart because their mRNA is present and they are important network links).

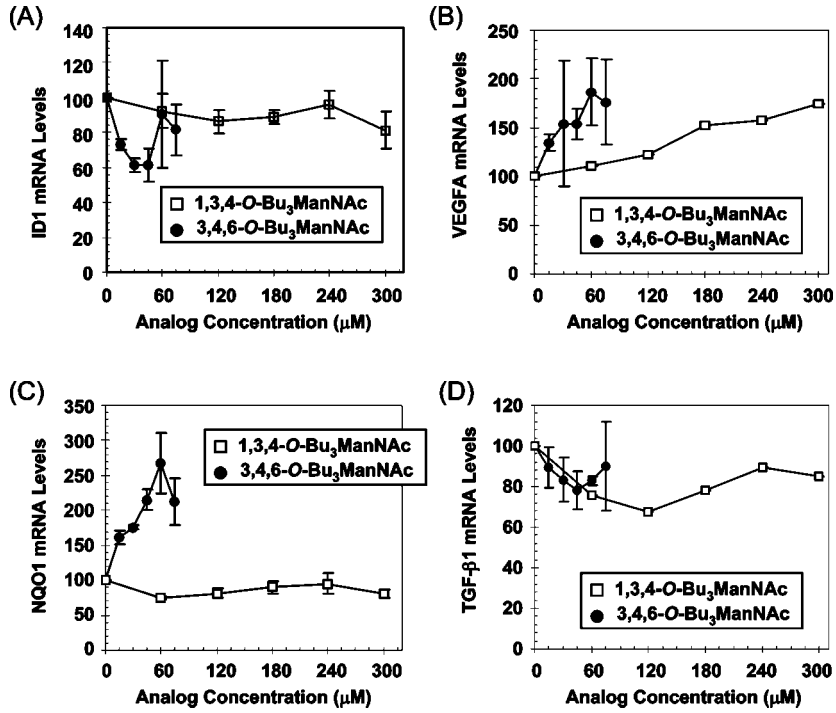

Figure 7. qRT-PCR validation of microarray targets. The levels of mRNA in MDA-MB-231 cells treated with 1,3,4-*O*-Bu_3ManNAc (**1c**) or 3,4,6-*O*-Bu_3ManNAc (**1b**) exposed to analogue for 3 days were monitored by qRT-PCR for ID1 (A), VEGFA (B), NQO1 (C), and TGF-β1 (D). Error bars represent SEM for independent experiments done at least in triplicate.

higher than the IC_{70} value for **1b** of 30 μM (which had been used in the microarray experiments to probe the onset of cytotoxicity) were monitored and the mRNA responses typically were amplified at 45 μM and sometimes at 60 μM. These trends often were reversed at 75 μM, which could be due to a biphasic gene regulatory response or the increasing toxicity at experienced at higher analogue levels. By contrast, comparable biphasic responses were not observed for **1c** even up to 300 μM (a detailed dose response including multiple concentrations between 0 and 75 μM (where **1b** elicited the greatest response) also showed no response for cells treated with **1c**; data not shown). Indeed, minimal changes of any type were observed for ID1, NQO1, or TGF-β1 and only a gradual increase was seen for VEGFA mRNA in cells treated with **1c**.

The qRT-PCR results provided verification that the changes in mRNA levels observed in the microarray experiments represented authentic changes in transcription and also strengthened the emerging paradigm that C6-acyl modified hexosamine analogues modulate genes important in the malignant transformation of human cells. To further explore the potential of analogues such as **1b** in cancer drug development, we next more thoroughly characterized the effects of this analogue on both mRNA (by qRT-PCR) and protein (by Western blots) levels for three molecular players (EGR1, TP53, and HPSE) involved in the network of cancer related genes shown in Figure 6 in MDA-MB-231 breast cancer cells and also in HCT-116 colon cancer cells. These experiments, reported in more detail below, established that the mRNA profiling provided a reliable means to identify genes affected by the analogues but nonetheless masked many of the nuances engendered by these compounds in cancer cells, as biphasic dose responses were typical, mRNA vs protein disparities existed for these genes, and the regulation of these genes was cell type- and time-dependent.

Evaluation of EGR1 in Analogue-Treated Cancer Lines. Because of the importance of EGR1 as a central player in the regulation of several oncogenes (for example, for the well-known and central player TP53[31]) we evaluated this gene in MDA-MB-231 and HCT-116 cells. First, **1b** was more toxic ($\sim$ 3-fold) in the latter line (Figure 8A), necessitating short time frames for analysis or low concentrations to avoid secondary effects related to toxicity. EGR1 mRNA levels strongly responded to **1b**, increasing about 2-fold at 45 μM and then spiking to as high as 25-fold versus control levels in some experiments at 60 and 75 μM (Figure 8B). Unexpectedly, however, the increase in EGR1 mRNA levels was not conveyed to the protein level (Figure 8C); Western analysis showed that instead of an increase in EGR1, a drop of 2-fold or more was consistently seen at concentrations above 45 μM **1b** (Figure 8D). Figure 8E shows another typical response to the analogues, namely, a time dependence where at certain time points (in this case, at 24 h for HCT-116 cells) up-regulation of EGR1 occurred followed by down-regulation at later time points (e.g., 3 d). Interestingly, similar to the MDA-MB-231 cells, proteins levels for EGR1 followed an inverse relationship to mRNA levels in cells incubated with **1b** at both time points (Figure 8F and Figure 8G, respectively, for 24 h and 3 days).

Evaluation of TP53 in Analogue-Treated Cancer Lines. On the basis of the importance of TP53 in cancer and its connections with EGR1,[31] we next analyzed the effects of butanoylated ManNAc analogues on this gene. When mRNA levels were monitored in MDA-MB-231 cells incubated with the inactive C6-OH analogue **1c**, results were variable from experiment to experiment but showed no convincing trend up to 300 μM (Figure 9A). By contrast, the active C1-OH analogue **1b** consistently suppressed TP53 at the mRNA level at 60 and 75 μM and also strongly down-regulated TP53 protein levels at lower analogue levels (e.g., at 15 μM) than required for mRNA inhibition. For the HCT-116 line at 24 h, **1b** had minimal impact at the mRNA level but elicited a biphasic diminution of protein at 20 μM that rebounded at higher concentrations (Figure 9B). After 3 days, TP53 mRNA levels in HCT-116 cells incubated with 15 μM or higher of **1b** were reduced, but again,

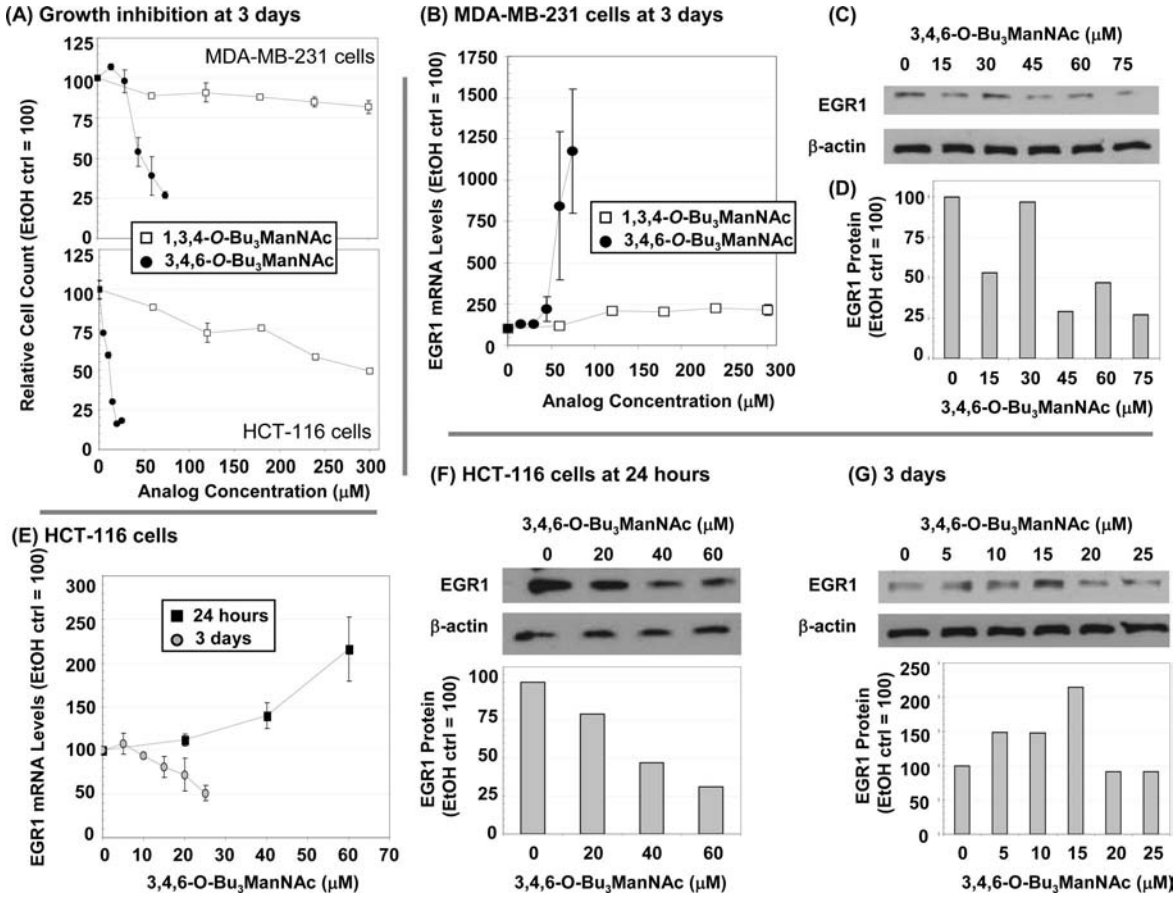

Figure 8. Effects of analogues on EGR1 showing time-, cell line-, concentration-, mRNA-, and protein-specific responses. (A) Growth inhibition of MDA-MB-231 and HCT-116 cells were monitored after 3 days of exposure to 1,3,4-*O*-Bu_3ManNAc (**1c**) or 3,4,6-*O*-Bu_3ManNAc (**1b**). (B) EGR1 mRNA levels were evaluated after 3 days of exposure to **1b** or **1c**, and corresponding protein levels are shown in panel C (with quantification of the bands by densitometry using the NIH ImageJ software, shown in panel D). (E) EGR1 mRNA levels are shown after 1 or 3 days of incubation with **1b**, and the corresponding protein levels are shown in panels F and G, respectively. At least three independent experiments were performed for each data set shown, with comparable results obtained each time, and error bars represent SEM. Representative Western blot data from one experiment are shown.

the impact at the protein level was considerably more pronounced with almost complete ablation at 20 and 25 μM (Figure 9C).

Although the primary objective of this paper was to evaluate the hexosamine template as a platform for drug discovery by characterizing SAR in the context of transcription, it is worth noting that the rudimentary analysis of proteins we conducted indicated that connections between the analogues and EGR1 and TP53 are stronger at the protein rather than at the mRNA levels. In particular, the correspondence between up-regulation of EGR1 mRNA under none of the conditions evaluated translated into increased TP53; instead the reduced protein levels of EGR1 qualitatively corresponded with the reduction in protein levels of TP53. Finally, of relevance to cancer, the changes to TP53 that were observed do not have an obvious correspondence to the growth inhibitory and proapoptotic nature of **1b**. One explanation could be that the gain-of-function mutant TP53 found in MDA-MB-231 cells[32] is tumor promoting;[33] therefore, its knockdown is beneficial toward killing the cancer cell. By contrast, TP53 in the HCT-116 cells is wild-type and it is difficult to explain the enhanced toxicity of **1b** in this cell line if TP53 is involved; it is likely, therefore, that **1b** acts by a TP53 independent mechanism in this line.

Evaluation of HPSE in Analogue-Treated Cancer Lines. As a final molecular target at the nexus of the proapoptotic and antimetastatic effects of analogues, we tested the impact of **1b** on heparanase (HPSE). In these experiments, no clear trends emerged at the mRNA levels for either the MDA-MB-231 cells at 3 days (Figure 10A) or for the HCT-116 cells at either 24 h (Figure 10B) or 3 d (Figure 10C). Dramatic changes at the protein level, however, were observed at the 3 day time point for both lines. Interestingly, in both lines these changes showed an inverse relationship to TP53; for example, at 20 and 25 μM **1b** in HCT-116 cells TP53 was dramatically reduced (to 5% or less) and HPSE was correspondingly increased (by 50-fold or more). Superficially, the gain in the prometastatic protein HPSE in cell treated with **1b** is at odds with the anti-invasive properties of this analogue. However, it is important to note that we monitored the latent 65 kDa form of HPSE, which subsequently requires proteolytic processing to a 50 kDa species that heterodimerizes with an 8 kDa form to gain activity.[34,35] Consequently, the increase in heparanase shown in Figure 10 may represent the accumulation of inactive protein within a cell with a concomitant reduction in the active form, consistent with the anti-invasive nature of **1b**.

Emerging Connections between Analogues and NF-κB Are Supported by AutoDock Modeling. At the outset of this project, two lines of evidence were available to explain the impact of SCFA−hexosamine analogues on transcription. First, the gene-regulatory HDACi properties of SCFA (contributed by *n*-butyrate liberated by *n*-butanoylated analogues such as Bu_4ManNAc (**1a**, Figure 1)) had been established over the past

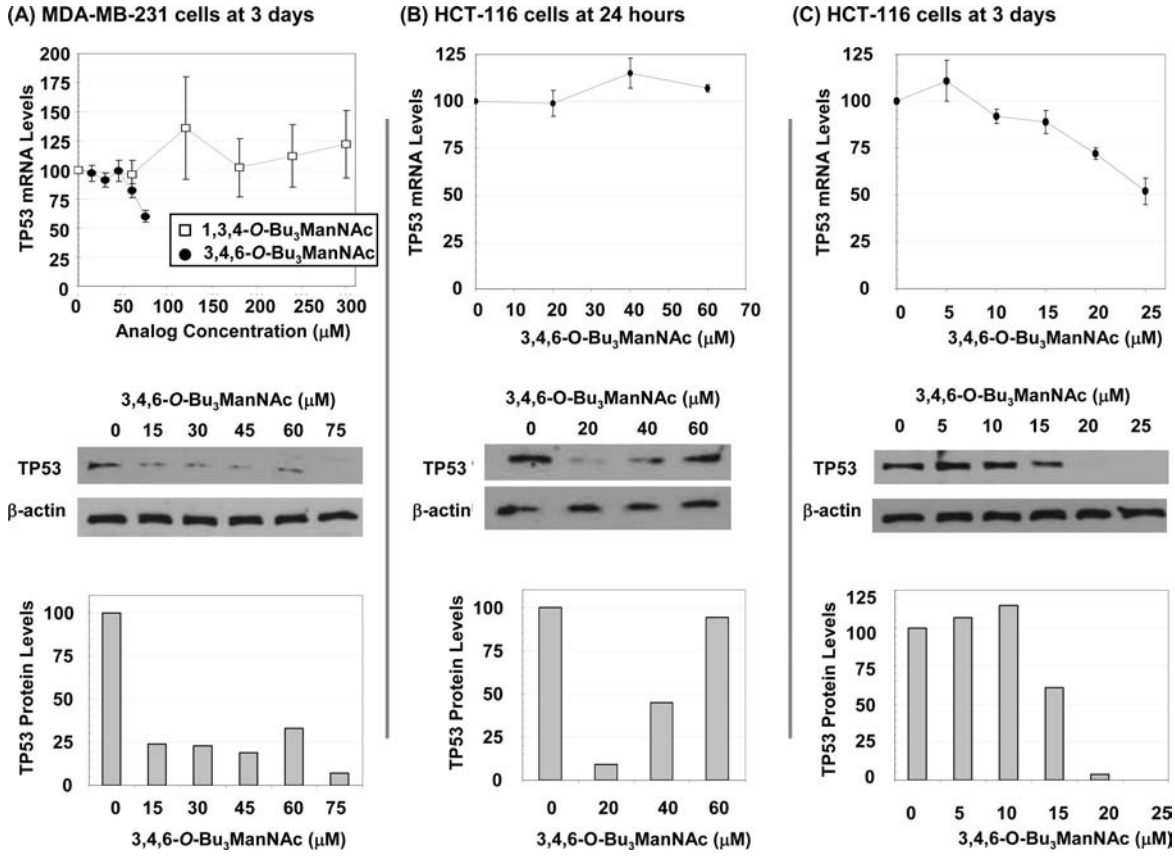

Figure 9. Effects of analogues on TP53 showing time-, cell line-, concentration-, mRNA-, and protein-specific responses. qRT-PCR was used to determine mRNA levels, and protein levels were analyzed by Western blots (and quantified by densitometry using the NIH ImageJ software) for MDA-MB-231 cells exposed to **1b** or **1c** for 3 d (A) or for HCT-116 cells exposed to **1b** for 24 h (B) or 3 d (C). At least three independent experiments were performed for each data set shown, with comparable results obtained each time, and error bars represent SEM. Representative Western blot data from one experiment are shown.

two decades (as reviewed by Sampathkumar and coauthors[36] and previous studies from our laboratory[5,6]). Second, recent evidence that changes in flux through the sialic acid pathway can modulate transcription[20] provided a second mechanism by which ManNAc-based analogues (e.g., **1a**−**h**) could regulate gene expression. However, the dramatically different genetic effects of tributanoylated ManNAc isomers (e.g., 1,3,4-*O*-Bu_3ManNAc, **1c**, and 3,4,6-*O*-Bu_3ManNAc, **1b**[4]) and similarly divergent responses to monobutanoylated, triacetylated ManNAc isomers (e.g., 6-*O*-Bu-1,3,4-*O*-Ac_3ManNAc, **1g**, and 1-*O*-Bu-3,4,6-*O*-Ac_3ManNAc, **1h**) indicated that critical regulatory facets of these analogues lay outside these two canonical HDACi and glycosylation activities, respectively. Consequently, the hypothesis that a third mode of "scaffold-dependent" activity of SCFA−hexosamine analogues exists (see Figure 1) that augments, or indeed dominates, HDACi- and sugar-based gene regulation helped solve the conundrum posed by the divergent activity of various acylated ManNAc analogues. An intriguing clue to the mechanism behind this newfound activity was provided by previously discovered, but tenuous, connections to NF-κB where analogues with "anticancer" activity inhibited this pathway (e.g., 3,4,6-*O*-Bu_3ManNAc, **1b**[5]) while high-flux analogues with negligible toxicity (e.g., 1,3,4-*O*-Bu_3ManNAc, **1c**[4]) did not.

In addition to strengthening the hypothesis that the gene regulatory activities of SCFA−hexosamine analogues are derived primarily from a "scaffold-dependent" mechanism, connections between several of the specific genes identified (e.g., those in the network shown in Figure 6 including ID1,[37,38] TP53,[39,40] and NQO1[41,42]) and NF-κB support the premise that this pathway plays a critical role in mediating cellular responses. Accordingly, as the final part of this report, we used computational modeling to support the nascent hypothesis that NF-κB effects do not occur through "obvious" mechanisms such as inhibition of proteasome activity[5] but instead through direct interaction with NF-κB proteins. Specifically, AutoDock modeling[43] was used to evaluate the binding of "active" analogues **1a** and **1b** to NFKB1 compared against the "inactive" analogue **1c**. As shown in Figure 11, all of these compounds bind to NFKB1 with physiologically significant affinities (when compared to the binding of sugar ligands to their natural protein targets, as tabulated by Laederach and Reilly[44]). Interestingly, **1b** binds to NFKB1 with ∼1 kcal/mol greater affinity than **1c**, which is a biologically relevant difference; **1a** and **1b** also bind in a different orientation where Gln279 is hydrogen-bond bound to the analogue compared to **1c**.

An important caveat to the docking results is that while they are consistent with the hypothesis that analogues with anticancer activities directly interact with elements of the NF-κB pathway, they do not rule out other mechanisms. For example, it is plausible that the analogues have multiple molecular targets, a premise that can only be evaluated by systematic docking of a library of analogues to all proteins within a cell. Because this endeavor is prohibitive because of both practical (access to adequate computational resources) and scientific (high resolution structural data are not available for many proteins) reasons, at present these results are intended to provide a foundation for the generation of hypotheses for experimental testing to confirm the putative NF-κB suppressive mechanism of SCFA−hexosamine drug candidates and also to gain new insights into this important therapeutic target. For example, the results obtained to date

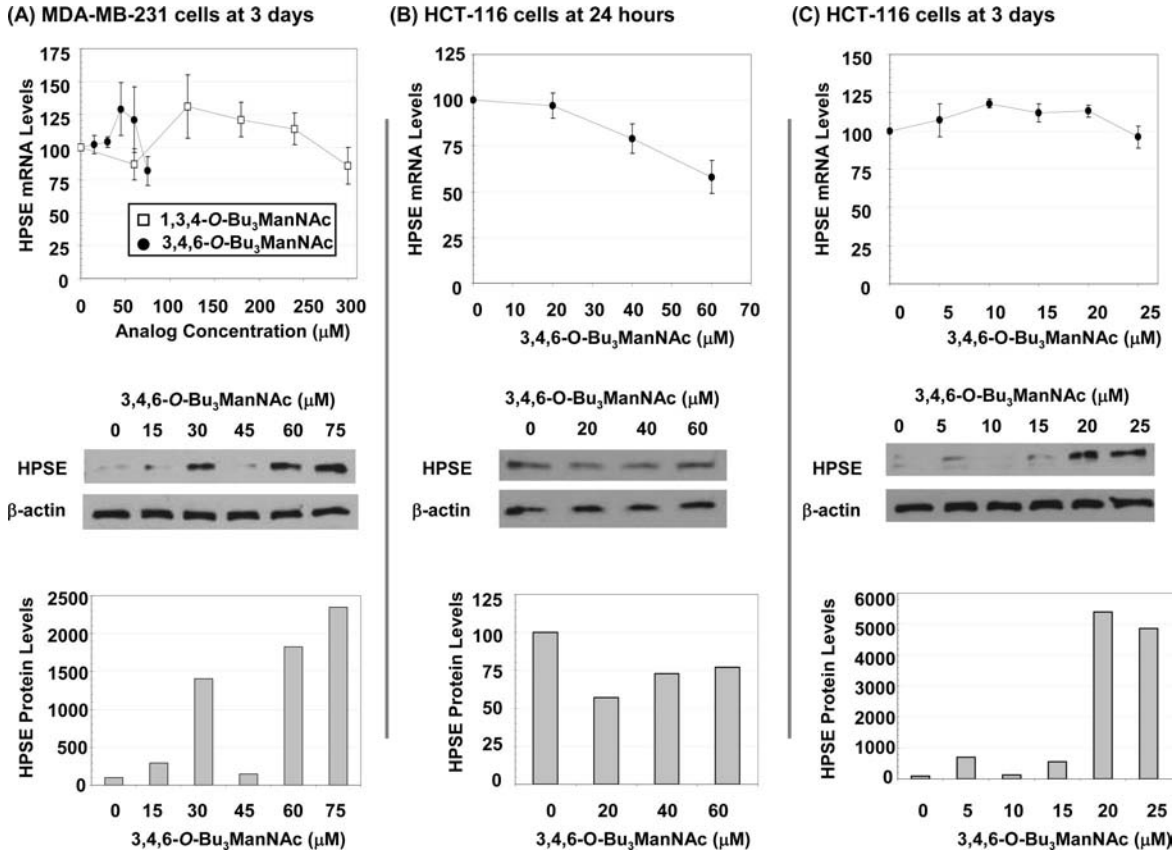

Figure 10. Effects of analogues on HPSE showing time-, cell line-, concentration-, mRNA-, and protein-specific responses. qRT-PCR was used to determine mRNA levels, and protein levels were analyzed by Western blots (and quantified by densitometry using the NIH ImageJ software) for MDA-MB-231 cells exposed to **1b** or **1c** for 3 d (A) or for HCT-116 cells exposed to **1b** for 24 h (B) or 3 d (C). At least three independent experiments were performed for each data set shown, with comparable results obtained each time, and error bars represent SEM. Representative Western blot data from one experiment are shown.

implicate the binding of analogue to Gln279 to be critical in suppressing NF−κB activities and site directed mutagenesis experiments could be used to test this possibility.

Concluding Comments

The results presented in this paper unambiguously establish the hexosamine to be a robust and surprisingly versatile template for modulating transcription and protein levels in cancer cells; as such, it thus constitutes an attractive platform for drug discovery (as outlined in Figure 2, literally tens of thousands of structures can be assembled from the basic natural hexosamines and SCFA). Clearly, much work remains to determine cell type specificity, the specific cellular targets that the analogues interact with, and whether these molecules engage a diverse set of receptors or a small set in various ways. Despite these ambiguities still afoot at this early stage of the development of these drug candidates, this report does establish several concrete and specific advances. From the angle of safety, which is a major concern of most chemotherapeutic agents, the idea that cancer drugs can be constructed of simple, nontoxic building blocks (which are regenerated during drug metabolism rather than an array of potentially toxic secondary metabolites) is appealing. Importantly, this report thoroughly establishes that the cellular responses elicited from drug metabolites (i.e., hexosamines and SCFA) are inconsequential compared to the template-dependent activities. From a narrow perspective, this report demonstrated that the analogues were capable of regulating several important oncogenes at both the transcriptional and protein levels in human cancer cells. Finally, from a broader perspective, this report supports the nascent hypothesis that SCFA−hexosamines modulate NF-κB, which has become an extremely important therapeutic target.[45−47]

Experimental Procedures

Analogue Synthesis, Characterization, and Storage. The starting materials *N*-acetyl-D-glucosamine (GlcNAc) and *N*-acetyl-D-galactosamine (GalNAc) were purchased from Sigma-Aldrich, and *N*-acetyl-D-mannosamine (ManNAc) was purchased from New Zealand Pharmaceuticals. The previously reported analogues 2-acetamido-2-deoxy-1,3,4,6-tetra-*O*-butanoyl-α,β-D-mannopyranose (Bu_4ManNAc, **1a**[6,13]), 2-acetamido-2-deoxy-1,3,4,6-tetra-*O*-acetyl-α,β-D-mannopyranose (Ac_4ManNAc, **1d**[48]), 2-acetamido-2-deoxy-3,4,6-tri-*O*-acetyl-α,β-D-mannopyranose (3,4,6-*O*-Ac_3ManNAc, **1f**[4]), 2-acetamido-2-deoxy-3,4,6-tri-*O*-butanoyl-α,β-D-mannopyranose (3,4,6-*O*-Bu_3ManNAc, **1b**[4]), 2-acetamido-2-deoxy-1,3,4-tri-*O*-butanoyl-α,β-D-mannopyranose (1,3,4-*O*-Bu_3ManNAc, **1c**[4]), 1,3,4,6-tetra-*O*-acetyl-2-deoxy-2-(4-oxopentanoyl)amino-α,β-D-mannopyranose (Ac_4ManNLev, **1e**[49]), and 2-acetamido-2-deoxy-3,4,6-tri-*O*-butanoyl-α,β-D-glucopyranose (3,4,6-*O*-Bu_3GlcNAc, **2a**[5]) were synthesized following the procedures in the cited references. The synthesis and characterization of the novel compounds 6-*O*-Bu-1,3,4-*O*-Ac_3ManNAc (**1g**), 1-*O*-Bu-3,4,6-*O*-Ac_3ManNAc (**1h**), and 3,4,6-*O*-Bu_3GalNAc (**3a**) are reported in detail in the Supporting Information (available online). Elemental analysis results of unreported compounds were obtained from Atlantic Microlab, Inc. (www.atlanticmicrolab.com), and **1g** had a purity of >98%, **1h** had >99%, and **3a** had >97%.

Commercial reagents, including solvents, used in analogue synthesis were used without further purification. Thin layer chromatography (TLC) was performed on silica gel coated glass plates

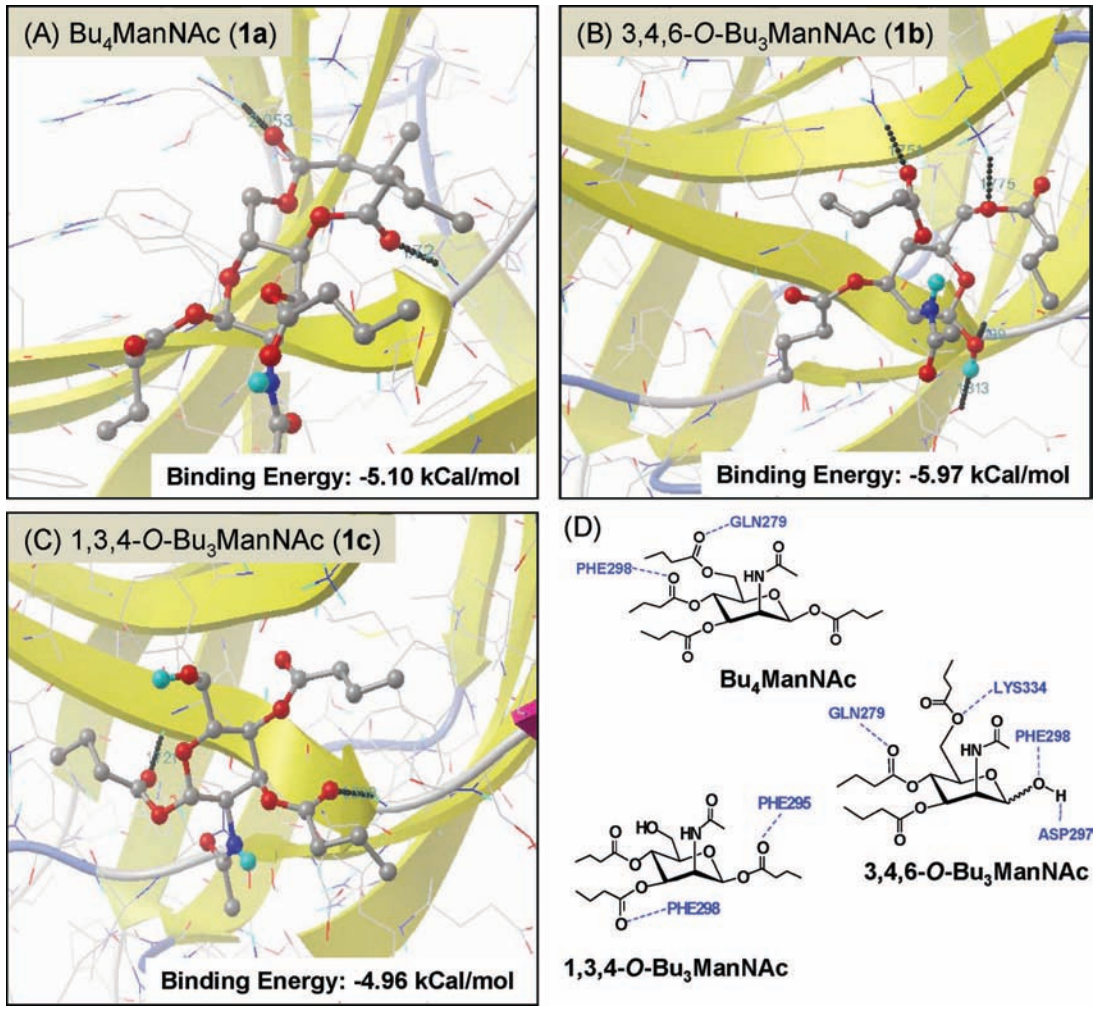

Figure 11. AutoDock-modeled binding of *n*-butanyolated ManNAc analogues to NFKB1. The best fit binding of **1a** (A), **1b** (B), or **1c** (C) to NFKB1 was determined by using the AutoDock 4.0 software tool. Annotation of hydrogen binding contacts is given in panel D.

(catalog no. 21521). Column chromatography was performed using 60 Å silica gel. NMR spectra (^{1}H and ^{13}C) were obtained using a 400 MHz Bruker instrument at 22 °C; the chemical shifts values are reported in "δ" and coupling constants (J) in Hz. Mass spectrometry was performed using ESI-MS, high resolution FAB-MS, or MALDI-TOF (Voyager DE-STR, Applied Biosystems). Molecular sieves, 4 Å, were activated at 150 °C overnight, cooled in a desiccator, and powdered freshly before use. Solvent evaporations were performed on a rotary evaporator under reduced pressure at 30−35 °C.

Stock solutions of analogues were typically made at a concentration of 50 mM in ethanol to maintain sterility and also because the SCFA-derivatized sugars typically were not soluble in aqueous solutions (e.g., in tissue culture media) above ∼500−700 μM. Analogues were either used directly in the cell culture experiments, or when volumes of less than 0.5 μL were required, a 10× dilution of the stock solutions was used. When stored at either 4 or −20 °C the analogues were stable in solution in ethanol for several months (i.e., migration of SCFA groups to the free hydroxyl of triacetylated or tributanoylated analogues was not observed). Analogues were used as the α,β mixtures obtained from column chromatography (typically, ∼90:10 α/β).

Cell Culture Conditions. MDA-MB-231 breast cancer cells and HCT116 colon cancer cells were obtained from the American Type Culture Collection (ATCC; Manassas, VA) and cultured in RPMI 1640 medium (Mediatech) and McCoy's 5A medium (Invitrogen), respectively. Culture medium was supplemented with 10% fetal bovine serum (FBS, Atlanta Biologicals). Cells were grown to 80% confluency in T-175 flasks (Sarstedt), trypsinized using TrypLE Express (Invitrogen), and subpassaged one or two times per week into T-175 flasks, six-well tissue culture (TC) plates, 10 cm TC plates, or T-75 flasks depending on the experiment (as described below). In all cases, cells were cultured at 37 °C in a water-saturated environment maintained at 5.0% CO_2.

For most experiments where cells were co-incubated with analogue, MDA-MB-231 breast cancer cells were plated in six-well tissue culture plates at a density of (2.0−2.7) × 10^5 cells/well and HCT-116 colon cancer cells were plated at a density of 1.0 × 10^5 cells/well. To each well, 3.0 mL of medium, the appropriate concentration of analogue dissolved in ethanol (or ethanol for the control samples, which was typically less than 0.5% v/v, a level that has no discernible effect on the end points evaluated in this study), and 1.0 mL of cell suspension were added. Cell numbers were determined using a Beckman Coulter Z2 Coulter particle count and size analyzer; two cell counts of 100 μL each were conducted for each sample. Unless otherwise indicated, the cells were grown for 3 days and then harvested for the subsequent biochemical assays.

Microarray Experiments and Data Analysis. The first set of experiments was performed with the Affymetrix GLYCOv3 chip using our previously described methodology to prepare the samples,[6] which were processed by the Consortium for Functional Glycomics (CFG) in triplicate for each sample (the microarray data are accessible at the CFG Web site http://www.functionalglycomics.org/static/index.shtml). Several criteria were considered to narrow the list of potential gene candidates. First, only human genes were considered (the chip includes both human and murine gene sequences). Second, because the call can be used as an indication of the reliability of the data, only those probe sets with "Present" call values were considered. Next, a Student t test was used to determine the list of statistically significant genes that were

Table 2. Primers Used in qRT-PCR Validation of cDNA Microarray Gene Leads

gene	forward primer (5′ → 3′)	reverse primer (5′ → 3′)
EGR1	TGACCGCAGAGTCTTTTCCT	TGGGTTGGTCATGCTCACTA
TP53	TGGCCATCTACAAGCAGTCACA	GCAAATTTCCTTCCACTCGGAT
HPSE	GTTCCTGTCCGTCACCATTGA	TTGGAGAACCCAGGAGGAT
NQO1	AAAGGACCCTTCCGGAGTAA	CCATCCTTCCAGGATTTGAA
ID1	CGGATCTGAGGGAGAACAAG	CTGAGAAGCACCAAACGTGA
VEGFA	AAGGAGGAGGGCAGAATCAT	ATCTGCATGGTGATGTTGGA
TGF-β1	CACGTGGAGCTGTACCAGAA	GAACCCGTTGATGTCCACTT
IL1R1	ATTGCAGGACACAAGCACAG	GTTCCTTCAAGCAGGCAAAG
GAPDH	CCACCCATGGCAAATTCC	GATGGGATTTCCATTGATGACA

Table 3. List of Antibodies Used in Western Blotting Analysis To Verify Protein Expression Levels of Microarray Gene Leads

protein	primary antibody	secondary antibody
EGR1 (82 kDa)	Santa Cruz (sc-110) rabbit, 1:1000 dilution	cell signaling technology (7074), 1:5000 dilution
TP53 (53 kDa)	Calbiochem (OP03) mouse, 1:100 dilution	cell signaling technology (7076), 1:10000 dilution
HPSE (65 kDa)	Abgent (AP1631a) rabbit, 1:200 dilution	cell signaling technology (7074), 1:25000 dilution
β-actin (42 kDa)	Sigma (A5316) mouse, 1:100000 dilution	cell signaling technology (7076), 1:10000 dilution

differentially expressed between two conditions: analogue-treated versus control. A cutoff *p*-value of 0.10 was used. Finally, mean signal values were compared for the ethanol controls and the experimental conditions. Only those probe sets with ratios greater than 1.25 or less than 0.80 were considered (i.e., |fold change (FC)| > 25%).

Subsequent array analysis was done using the Affymetrix Human Genome U133 2.0 Plus chip by using the protocols and facilities available through the Johns Hopkins Cancer Center Microarray Core. These data have been deposited in NCBI's Gene Expression Omnibus[50] and are accessible through GEO series accession number GSE11407 (http://www.ncbi.nlm.nih.gov/geo/query/acc.cgi?acc=GSE11407). In the analysis of the data from these experiments, several criteria were used to determine "actual" differences between the control samples and the experimental samples. First, only those probe sets that contained a call of "Present" for all samples submitted were considered. Second, a Student's *t* test was conducted on the signal values between the ethanol control samples and each condition. A cutoff *p*-value of 0.05 was used to determine statistically significant differences in gene expression levels. Third, only sample-versus-control ratios greater than 1.50 or less than 0.67 were considered (i.e., |FC| > 50%). Probe sets that met these criteria were considered statistically significant. In some of the analyses, a less stringent ratio cutoff was used: greater than 1.25 or less than 0.80 (|FC| > 25%). The less stringent cutoff is indicated in these cases.

To gain insight into the biological implications, the list of probe sets (genes) that met the aforementioned criteria was then further investigated using pathway analysis software. Pathway Express (http://vortex.cs.wayne.edu/projects.htm),[28] an online software tool, was used to determine significant pathways. A comprehensive gene list was generated that included all genes with a |FC| > 50% for at least one analogue. This comprehensive gene list was used as the input gene list for the Pathway Express analysis conducted to identify key pathways. Once key pathways were determined ($p < 0.10$), a comprehensive gene list containing all genes with |FC| > 25% for at least one analogue was used to identify the maximum number of affected genes in these pathways.

Quantitative Real Time Polymerase Chain Reaction (qRT-PCR). RNA was isolated using TRIzol reagent (Invitrogen) following manufacturer's instructions. Samples were either processed immediately or frozen at −80 °C for later processing. Isolated RNA was then purified using TURBO DNase (Ambion) followed by RNEasy Spin Columns (Qiagen) following the manufacturer's instructions. OD_{260} and OD_{280} readings were conducted using a Beckman DU 530 Life Science UV/visible spectrophotometer to determine the concentration and purity of the RNA samples. Purified RNA samples were reverse-transcribed to cDNA (cDNA) using a Bio-Rad iCycler and the SuperScript III first strand synthesis kit (Invitrogen), following the manufacturer's instructions. Newly synthesized cDNA was diluted 5-fold in TE buffer and used immediately for qRT-PCR analysis or frozen at −20 °C for later use.

Polymerase chain reactions (PCR) were carried out in 96-well plates with each sample analyzed in quadruplicate. A primer mixture containing 11.4 μL of Roche FastStart SYBR Green Master Mix, 1.0 μL of forward primer (10 μM), 1.0 μL of reverse primer (10 μM; the sequences of the primers are given in Table 2), and 8.6 μL of DEPC water was loaded into each well, followed by 1.0 μL of the cDNA sample. The plate was loaded into an ABI Prism 7700 sequence detector, and the following program was run: initial cycle at 95 °C for 10 min, followed by 40 cycles of 95 °C for 15 s and then 60 °C for 1.0 min. The relative gene expression levels were determined using the $\Delta\Delta C_t$ method ($2^{-\Delta\Delta C_t}$),[51,52] in which the cycle number for a specific experimental sample and gene is normalized to both the housekeeping gene control (GAPDH for all these studies) and the experimental control (ethanol control for concentration dependence studies or the Time = 0 h control for time dependence studies).

Protein Determination by Western Analysis. Western blot analysis was performed to determine protein expression levels. Cells were harvested after 3 days (except where indicated) and washed twice with ice-cold phosphate-buffered saline (PBS) and lysed using ≤400 μL of RIPA buffer (Sigma) supplemented with 1.0% protease inhibitor cocktail (Sigma) following the manufacturer's instructions. The total protein content was determined using the BCA assay (Pierce), and an equal mass (5−20 μg) of protein was loaded onto a polyacrylamide gel for each sample (high concentration samples were supplemented with Milli-Q water to attain equal concentrations for all samples) after mixing with an equal volume of Laemmli sample buffer (Bio-Rad, supplemented with 5.0% β-mercaptoethanol). Samples were heated for 5.0 min at 90 °C before being loaded in a 4.0−15% Tris-HCl gel (Bio-Rad). The gel was electrophoresed in a Mini Protean 3 cell (Bio-Rad) at 70 V for 15 min and then at 100 V for 45−60 min. Once complete, the gel was transferred to a Trans-Blot transfer medium nitrocellulose membrane (Bio-Rad) by loading into a Mini Trans-Blot cell (Bio-Rad) and electrophoresed at 250 mA for 60 min at 0 °C (i.e., in ice). The membrane was subsequently blocked for 1.0 h in 5.0% w/v blocking grade milk (blotting grade blocker nonfat dry milk (Bio-Rad) in TBST (Tris-buffered saline Tween-20; 0.1% Tween-20 in TBS)). The membrane was incubated with primary antibody diluted in 5.0% milk for 2.0 h at room temperature or overnight at 4.0 °C. After being washed three times with TBST, the membrane was incubated with secondary antibody diluted in 5.0% milk for 1.0 h at room temperature. The membrane was washed five times with TBST before being exposed to SuperSignal West Dura chemiluminescent reagent (Pierce). After 5.0 min of exposure, the membrane was covered with a clear sheet protector and sealed in a developing cassette. Films were developed by exposing film to the membrane and developing in developer, washer, and fixer for 7 s each. Protein expression levels were determined by quantifying

band darkness using NIH ImageJ software.[52] β-Actin housekeeping protein was used to verify equal protein loading and to normalize protein expression levels. Two independent experiments were performed for Western blot analysis of the proteins of interest. Table 3 lists the antibodies and dilutions used in this study. The TP53 OP03 antibody detects both wild-type and mutant forms of the protein. The HPSE AP1631a antibody detects the N-terminus of the protein, which is present in the latent 65 kDa form of the enzyme but is cleaved in the active form of the protein (a 50 + 8 kDa heterodimer).

AutoDock Modeling. The protein structure for NFKB1 (PDB code 1bSF) was obtained from the RCSB Protein Data Bank (PDB, http://www.rcsb.org/) and imported into the AutoDock Tools v1.5.2r2 (Molecular Graphics Laboratory, The Scripps Research Institute, La Jolla, CA)[43] program. The files containing analogue structures were generated in three steps. First, chemical structures were created by ChemDraw (CambridgeSoft). Then the SMILES form of the structure was copied and pasted into the Web site (http://www.molecular-networks.com/online_demos/ corina_demo.html), and finally PDB files were downloaded and imported to AutoDock. A detailed explanation of this protocol is provided in the Supporting Information.

Acknowledgment. Funding was provided by the National Institutes of Health (Grant CA112314-01 for ManNAc analogue synthesis and accompanying biological testing and Grant AR054005-01 for GlcNAc and GalNAc synthesis and evaluation). We are grateful to the Olson Laboratory (The Scripps Research Institute, La Jolla, CA) for assistance with the AutoDock modeling experiments.

Supporting Information Available: Synthesis and characterization of analogueues and the protocol followed for AutoDock modeling. This material is available free of charge via the Internet at http://pubs.acs.org.

References

(1) Keppler, O. T.; Horstkorte, R.; Pawlita, M.; Schmidt, C.; Reutter, W. Biochemical engineering of the *N*-acyl side chain of sialic acid: biological implications. *Glycobiology* **2001**, *11*, 11R–18R.
(2) Campbell, C. T.; Sampathkumar, S.-G.; Weier, C.; Yarema, K. J. Metabolic oligosaccharide engineering: perspectives, applications, and future directions. *Mol. BioSyst.* **2007**, *3*, 187–194.
(3) Aich, U.; Yarema, K. J. Metabolic Oligosaccharide Engineering: Perspectives, Applications, and Future Directions. In *Glycosciences*, 2nd ed.; Fraser-Reid, B., Tatsuta, K., Thiem, J., Eds.; Springer-Verlag: Berlin, 2008; pp 2136−2190.
(4) Aich, U.; Campbell, C. T.; Elmouelhi, N.; Weier, C. A.; Sampathkumar, S.-G.; Choi, S. S.; Yarema, K. J. Regioisomeric SCFA attachment to hexosamines separates metabolic flux from cytotoxcity and MUC1 suppression. *ACS Chem. Biol.* **2008**, *3*, 230–240.
(5) Campbell, C. T.; Aich, U.; Weier, C. A.; Wang, J. J.; Choi, S. S.; Wen, M. M.; Maisel, K.; Sampathkumar, S.-G.; Yarema, K. J. Targeting pro-invasive oncogenes with short chain fatty acid−hexosamine analogs inhibits the mobility of metastatic MDA-MB-231 breast cancer cell. *J. Med. Chem.* **2008**, *51*, 8135–8147.
(6) Sampathkumar, S.-G.; Jones, M. B.; Meledeo, M. A.; Campbell, C. T.; Choi, S. S.; Hida, K.; Gomutputra, P.; Sheh, A.; Gilmartin, T.; Head, S. R.; Yarema, K. J. Targeting glycosylation pathways and the cell cycle: sugar-dependent activity of butyrate−carbohydrate cancer prodrugs. *Chem. Biol.* **2006**, *13*, 1265–1275.
(7) Keller, T. H.; Pichota, A.; Yin, Z. A practical view of "druggability". *Curr. Opin. Chem. Biol.* **2006**, *10*, 357–361.
(8) Dove, A. The bittersweet promise of glycobiology. *Nat. Biotechnol.* **2001**, *19*, 913–917.
(9) Fuster, M. M.; Esko, J. D. The sweet and sour of cancer: glycans as novel therapeutic targets. *Nat. Rev. Cancer* **2005**, *5*, 526–542.
(10) Meutermans, W.; Le, G. T.; Becker, B. Carbohydrates as scaffolds in drug discovery. *ChemMedChem* **2006**, *1*, 1164–1194.
(11) Lipinski, C.; Hopkins, A. Navigating chemical space for biology and medicine. *Nature (London)* **2004**, *432*, 855–861.
(12) Lavis, L. D. Ester bonds in prodrugs. *ACS Chem. Biol.* **2008**, *3*, 203–206.
(13) Kim, E. J.; Sampathkumar, S.-G.; Jones, M. B.; Rhee, J. K.; Baskaran, G.; Yarema, K. J. Characterization of the metabolic flux and apoptotic effects of *O*-hydroxyl- and *N*-acetylmannosamine (ManNAc) analogs in Jurkat (human T-lymphoma-derived) cells. *J. Biol. Chem.* **2004**, *279*, 18342–18352.
(14) Luchansky, S. J.; Yarema, K. J.; Takahashi, S.; Bertozzi, C. R. GlcNAc 2-epimerase can serve a catabolic role in sialic acid metabolism. *J. Biol. Chem.* **2003**, *278*, 8036–8042.
(15) Kim, E. J.; Jones, M. B.; Rhee, J. K.; Sampathkumar, S.-G.; Yarema, K. J. Establishment of *N*-acetylmannosamine (ManNAc) analogue-resistant cell lines as improved hosts for sialic acid engineering applications. *Biotechnol. Prog.* **2004**, *20*, 1674–1682.
(16) Jones, M. B.; Teng, H.; Rhee, J. K.; Baskaran, G.; Lahar, N.; Yarema, K. J. Characterization of the cellular uptake and metabolic conversion of acetylated *N*-acetylmannosamine (ManNAc) analogues to sialic acids. *Biotechnol. Bioeng.* **2004**, *85*, 394–405.
(17) Mahal, L. K.; Yarema, K. J.; Bertozzi, C. R. Engineering chemical reactivity on cell surfaces through oligosaccharide biosynthesis. *Science* **1997**, *276*, 1125–1128.
(18) Yarema, K. J.; Mahal, L. K.; Bruehl, R. E.; Rodriguez, E. C.; Bertozzi, C. R. Metabolic delivery of ketone groups to sialic acid residues. Application to cell surface glycoform engineering. *J. Biol. Chem.* **1998**, *273*, 31168–31179.
(19) Williams, E. A.; Coxhead, J. M.; Mathers, J. C. Anti-cancer effects of butyrate: use of micro-array technology to investigate mechanisms. *Proc. Nutr. Soc.* **2003**, *62*, 107–115.
(20) Kontou, M.; Bauer, C.; Reutter, W.; Horstkorte, R. Sialic acid metabolism is involved in the regulation of gene expression during neuronal differentiation of PC12 cells. *Glycoconjugate J.* **2008**, *25*, 237–244.
(21) Murrell, M. P.; Yarema, K. J.; Levchenko, A. The systems biology of glycosylation. *ChemBioChem* **2004**, *5*, 1334–1447.
(22) Krambeck, F. J.; Betenbaugh, M. J. A mathematical model of *N*-linked glycosylation. *Biotechnol. Bioeng.* **2005**, *92*, 711–728.
(23) Lau, K. S.; Partridge, E. A.; Grigorian, A.; Silvescu, C. I.; Reinhold, V. N.; Demetriou, M.; Dennis, J. W. Complex *N*-glycan number and degree of branching cooperate to regulate cell proliferation and differentiation. *Cell* **2007**, *129*, 123–134.
(24) Gabius, H.-J.; Siebert, H.-C.; André, S.; Jiménez-Barbero, J.; Rüdiger, H. Chemical biology of the sugar code. *ChemBioChem* **2004**, *5*, 740–764.
(25) Lau, K. S.; Dennis, J. W. *N*-Glycans in cancer progress. *Glycobiology* **2008**, *18*, 750–760.
(26) Zanghi, J. A.; Mendoza, T. P.; Schmelzer, A. E.; Knop, R. H.; Miller, W. M. Role of nucleotide sugar pools in the inhibition of NCAM polysialylation by ammonia. *Biotechnol. Prog.* **1998**, *14*, 834–844.
(27) Basson, M. D.; Liu, Y.-W.; Hanly, A. M.; Emenaker, N. J.; Shenoy, S. G.; Gould Rothberg, B. E. Identification and comparative analysis of human colonocyte short-chain fatty acid response genes. *J. Gastrointest. Surg.* **2000**, *4*, 501–512.
(28) Khatri, P.; Sellamuthu, S.; Malhotra, P.; Amin, K.; Done, A.; Draghici, S. Recent additions and improvements to the Onto-Tools. *Nucleic Acids Res.* **2005**, *33*, W762–W765.
(29) Sampathkumar, S.-G.; Li, A. V.; Jones, M. B.; Sun, Z.; Yarema, K. J. Metabolic installation of thiols into sialic acid modulates adhesion and stem cell biology. *Nat. Chem. Biol.* **2006**, *2*, 149–152.
(30) Fong, S.; Debs, R. J.; Desprez, P.-Y. Id genes and proteins as promising targets in cancer therapy. *Trends Mol. Med.* **2004**, *10*, 387–392.
(31) Baron, V.; Adamson, E. D.; Calogero, A.; Ragona, G.; Mercola, D. The transcription factor Egr1 is a direct regulator of multiple tumor suppressors including TGFβ1, PTEN, p53, and fibronectin. *Cancer Gene Ther.* **2006**, *13*, 115–124.
(32) Hui, L.; Zheng, Y.; Yan, Y.; Bargonetti, J.; Foster, D. A. Mutant p53 in MDA-MB-231 breast cancer cells is stabilized by elevated phospholipase D activity and contributes to survival signals generated by phospholipase D. *Oncogene* **2006**, *25*, 7305–7310.
(33) Kim, E.; Giese, A.; Deppert, W. Wild-type p53 in cancer cells: when a guardian turns into a blackguard. *Biochem. Pharmacol.* **2009**, *77*, 11–20.
(34) Vlodavsky, I.; Elkin, M.; Abboud-Jarrous, G.; Levi-Adam, F.; Fuks, L.; Shafat, I.; Ilan, N. Heparanase: one molecule with multiple functions in cancer progression. *Connect. Tissue Res.* **2008**, *49*, 207–210.
(35) Vlodavsky, I.; Goldshmidt, O.; Zcharia, E.; Metzger, S.; Chajek-Shaul, T.; Atzmon, R.; Guatta-Rangini, Z.; Friedmann, Y. Molecular properties and involvement of heparanase in cancer progression and normal development. *Biochimie* **2001**, *83*, 831–839.
(36) Sampathkumar, S.-G.; Campbell, C. T.; Weier, C.; Yarema, K. J. Short-chain fatty acid-hexosamine cancer prodrugs: The sugar matters! *Drugs Future* **2006**, *31*, 1099–1116.
(37) Ling, M. T.; Wang, X.; Ouyang, X. S.; Xu, K.; Tsao, S. W.; Wong, Y. C. Id-1 expression promotes cell survival through activation of NF-κB signalling pathway in prostate cancer cells. *Oncogene* **2003**, *22*, 4498–4508.
(38) Yang, Y.; Liou, H. C.; Sun, X. H. Id1 potentiates NF-kappaB activation upon T cell receptor signaling. *J. Biol. Chem.* **2006**, *281*, 34989–34996.

(39) Lee, T. L.; Yang, X. P.; Yan, B.; Friedman, J.; Duggal, P.; Bagain, L.; Dong, G.; Yeh, N. T.; Wang, J.; Zhou, J.; Elkahloun, A.; Van Waes, C.; Chen, Z. A novel nuclear factor-κB gene signature is differentially expressed in head and neck squamous cell carcinomas in association with TP53 status. *Clin. Cancer Res.* **2007**, *13*, 5680–5691.

(40) Tergaonkar, V.; Perkins, N. D. p53 and NF-κB crosstalk: IKKα tips the balance. *Mol. Cell* **2007**, *26*, 158–159.

(41) Ahn, K. S.; Sethi, G.; Jain, A. K.; Jaiswal, A. K.; Aggarwal, B. B. Genetic deletion of NAD(P)H:quinone oxidoreductase 1 abrogates activation of nuclear factor-κB, IκBα kinase, c-Jun N-terminal kinase, Akt, p38, and p44/42 mitogen-activated protein kinases and potentiates apoptosis. *J. Biol. Chem.* **2006**, *281*, 19798–19808.

(42) Korashy, H. M.; El-Kadi, A. O. NF-κB and AP-1 are key signaling pathways in the modulation of NAD(P)H:quinone oxidoreductase 1 gene by mercury, lead, and copper. *J. Biochem. Mol. Toxicol.* **2008**, *22*, 274–283.

(43) Rosenfeld, R. J.; Goodsell, D. S.; Musah, R. A.; Morris, G. M.; Goodin, D. B.; Olson, A. J. Automated docking of ligands to an artificial active site: augmenting crystallographic analysis with computer modeling. *J. Comput.-Aided Mol. Des.* **2003**, *17*, 525–536.

(44) Laederach, A.; Reilly, P. J. Specific empirical free energy function for automated docking of carbohydrates to proteins. *J. Comput. Chem.* **2003**, *24*, 1748–1757.

(45) Calzado, M. A.; Bacher, S.; Schmitz, M. L. NF-κB inhibitors for the treatment of inflammatory diseases and cancer. *Curr. Med. Chem.* **2007**, *14*, 367–376.

(46) Okamoto, T.; Sanda, T.; Asamitsu, K. NF-κB signaling and carcinogenesis. *Curr. Pharm. Des.* **2007**, *13*, 447–462.

(47) Gilmore, T. D.; Herscovitch, M. Inhibitors of NF-κB signaling: 785 and counting. *Oncogene* **2006**, *25*, 6887–6899.

(48) Sampathkumar, S.-G.; Li, A. V.; Yarema, K. J. Synthesis of non-natural ManNAc analogs for the expression of thiols on cell surface sialic acids. *Nat. Protoc.* **2006**, *1*, 2377–2385.

(49) Jacobs, C. L.; Goon, S.; Yarema, K. J.; Hinderlich, S.; Hang, H. C.; Chai, D. H.; Bertozzi, C. R. Substrate specificity of the sialic acid biosynthetic pathway. *Biochemistry* **2001**, *40*, 12864–12874.

(50) Edgar, R.; Domrachev, M.; Lasha, A. E. Gene Expression Omnibus: NCBI gene expression and hybridization array data repository. *Nucleic Acids Res.* **2002**, *30*, 207–210.

(51) Livak, K. J.; Schmittgen, T. D. Analysis of relative gene expression data using real-time quantitative PCR and the $2^{-\Delta\Delta CT}$ method. *Methods* **2001**, *25*, 402–408.

(52) Wang, Z.; Sun, Z.; Li, A. V.; Yarema, K. J. Roles for GNE outside of sialic acid biosynthesis: modulation of sialyltransferase and BiP expression, GM3 and GD3 biosynthesis, proliferation and apoptosis, and ERK1/2 phosphorylation. *J. Biol. Chem.* **2006**, *281*, 27016–27028.

JM801661M